

University of Nebraska - Lincoln

DigitalCommons@University of Nebraska - Lincoln

Engineering Mechanics Dissertations & Theses

Mechanical & Materials Engineering,
Department of

12-2010

ANOMALOUS LOSS OF TOUGHNESS OF WORK TOUGHENED POLYCARBONATE

Shawn E. Meagher

University of Nebraska-Lincoln, shawn.meagher@gmail.com

Follow this and additional works at: <https://digitalcommons.unl.edu/engmechdiss>



Part of the [Engineering Mechanics Commons](#), [Mechanical Engineering Commons](#), and the [Mechanics of Materials Commons](#)

Meagher, Shawn E., "ANOMALOUS LOSS OF TOUGHNESS OF WORK TOUGHENED POLYCARBONATE"
(2010). *Engineering Mechanics Dissertations & Theses*. 14.

<https://digitalcommons.unl.edu/engmechdiss/14>

This Article is brought to you for free and open access by the Mechanical & Materials Engineering, Department of at DigitalCommons@University of Nebraska - Lincoln. It has been accepted for inclusion in Engineering Mechanics Dissertations & Theses by an authorized administrator of DigitalCommons@University of Nebraska - Lincoln.

ANOMALOUS LOSS OF TOUGHNESS OF WORK TOUGHENED
POLYCARBONATE

by

Shawn E. Meagher

A THESIS

Presented to the Faculty of
The Graduate College at the University of Nebraska
In Partial Fulfillment of Requirements
For the Degree of Master of Science

Major: Engineering Mechanics

Under the Supervision of Professor Mehrdad Negahban and Professor Joseph Turner

Lincoln, Nebraska

December, 2010

ANOMALOUS LOSS OF TOUGHNESS OF WORK TOUGHENED POLYCARBONATE

Shawn Edward Meagher, M.S.

University of Nebraska, 2010

Advisers: Mehrdad Negahban and Joseph Turner

Glassy polymers such as polycarbonate (PC) can be toughened through compressive plastic deformation. The increase in toughness is substantial, showing as much as a fifteen fold increase in the amount of dissipated energy during failure for samples compressed to 50% plastic strain. This toughness increase can be reversed through thermal aging at temperatures below the glass transition temperature ($T_g = 147^\circ\text{C}$).

The combined effect of plastic compression and thermal aging has been studied using Charpy, Single Edge Notch Bending (SENB), and Compact Tension (CT) tests. The tests mapped the response of samples cut along different orientations relative to the plastic compression as a function of plastic compression, thermal aging temperature and aging time. The Charpy and SENB tests were conducted on as received samples of PC that were 0%, 25% and 50% plastically compressed. The CT tests were done on annealed and quenched samples that were then compressed up to 35%. The Charpy samples were aged at isothermal temperatures between 105°C and 135°C . The SENB samples were aged at 105°C and 125°C . The CT samples were aged at 125°C . All samples were tested at room temperature. Three modes of failure were observed for the fracture surfaces, a low energy dissipation brittle fracture, high energy dissipation ductile fracture, and a mixed mode intermediate fracture. Toughening through plastic compression changed the failure mode of the PC from an initial low energy dissipation brittle fracture to an

intermediate or high energy dissipation failure. Thermal aging reversed this process in some cases. This effect was mapped as a function of sample orientation, aging temperature and aging time.

The dynamic Charpy test results were supported by the quasi-static SENB and CT results. The CT samples were small enough to provide samples in the third orientation, which had cracks propagating orthogonal to the direction of compression with crack surfaces that had a normal along the direction of compression. These samples failed with extremely low energy dissipation indicating that even though the compression improved the energy dissipation along the other two directions substantially (i.e., 5 to 15 times), it also resulted in a “weak” orientation.

Acknowledgement

I would first like to thank my advisers Mehrdad Negahban and Joseph Turner here at the UNL and Laurent Delbreilh and Jean Marc Saiter at the Université de Rouen. Their guidance and support has been instrumental to my success in this graduate program. I would also like to thank David Allen for introducing me to the international programs at UNL. Because of these men, I have been blessed with many opportunities that have helped me grow not only as an engineer, but also as a person.

I also would like to thank the Army Research Lab for partially funding this project; as well as the Department of Education and FACE-PUF for their support.

Finally, I would like to thank my parents, Michael and Judy, and my siblings. Without their loving support and encouragement, none of this would have been possible.

Table of Contents

Acknowledgement.....	iv
Table of Figures	vi
Chapter 1. Introduction	1
1.1 Polycarbonate.....	2
1.2 Previous Work	5
1.3 Tests Performed	7
Chapter 2. Sample Preparation.....	9
2.1 Pretreatment	9
2.2 Compression	10
2.3 Thermal Aging	11
2.4 Sample Machining	11
Chapter 3. Charpy Impact Tests.....	18
3.1 Introduction.....	18
3.2 Procedure	18
3.3 Results.....	21
3.4 Discussion.....	30
Chapter 4. Single Edged Notched Bending	35
4.1 Introduction.....	35
4.2 Procedure	35
4.3 Results.....	38
4.4 Discussion.....	45
Chapter 5. Compact Tension Tests	48
5.1 Introduction.....	48
5.2 Procedure	49
5.3 Results.....	53
5.4 Discussion.....	56
Chapter 6. Summary and Conclusion	58
Appendix A.....	61
SENB Load/Displacement Figures	61
Appendix B	64
CT Load/Displacement Figures	64
References.....	70

Table of Figures

Figure 1: PC monomer [2].	2
Figure 2: Exaggerated change in orientation of PC polymer chains	3
Figure 3: Anisotropy of ultrasonic wave modulus measured in plastically compressed PC Samples [5].	5
Figure 4: Uncompressed PC sheets & 50% (left) & 25% (right) compressed PC bars used to prepare charpy & SENB samples	10
Figure 5: Compressed PC cylinders used to prepare CT samples, from left to right: 0%, 15%, 25%, 35% & 40% compression.	11
Figure 6: Charpy sample geometry & notch diagram.	12
Figure 7: SENB sample geometry & notch diagram	13
Figure 8: TA & TT sample orientations for Charpy & SENB samples.	14
Figure 9: CT sample geometry & notch diagram.	15
Figure 10: Crack notching of CT sample with a razor blade.	16
Figure 11: AT, TT and TA Orientations of CT Samples	17
Figure 12: Charpy Testing Machine (CEAST 6545)	20
Figure 13: Charpy Sample Mount & Impact Hammer	20
Figure 14: Fracture Surface of Brittle Samples	22
Figure 15: Fracture Surface of Samples with Mixed Mode Failure (Shearing & Tensile Failure)	22
Figure 16: Fracture Surface of Ductile Samples.	23
Figure 17: Energy dissipation of Charpy samples aged at 105°C. Combined data from Strabala [1] and Meagher.	24
Figure 18: Energy dissipation of Charpy samples Aged at 125°C. Combined data from Strabala [1] and Meagher.	25
Figure 19: Energy dissipation of individual Charpy samples in the transition zone (25% TA, 125°C aging). Combined Data from Strabala [1] and Meagher.	27
Figure 20: Energy dissipation of individual Charpy samples in the transition zone (25% TT, 125°C aging). Combined Data from Strabala [1] and Meagher.	29

Figure 21: Failure mode of Charpy tests as a function of aging time and temperature. ...	30
Figure 22: SENB Testing Apparatus	36
Figure 23: Energy dissipation of SENB samples Aged at 105°C. Combined data from Strabala [1] and Meagher.....	38
Figure 24: Energy dissipation of SENB samples aged at 125°C. Combined data from Strabala [1] and Meagher.....	38
Figure 25: Load-displacement curves for each failure type.	39
Figure 26: Corrected load-line displacement at failure of SENB samples aged at 105°C. Combined data from Strabala [1] and Meagher.....	41
Figure 27: Corrected load-line displacement at failure of SENB samples aged at 125°C. Combined data from Strabala [1] and Meagher.....	41
Figure 28: Crack tip opening displacement at failure of SENB samples Aged at 105°C. Combined data from Strabala [1] & Meagher.	43
Figure 29: Crack tip opening displacement at failure of SENB samples aged at 125°C. Combined data from Strabala [1] & Meagher.	43
Figure 30: Data correction test on un-notched CT sample.....	50
Figure 31: CT testing apparatus.....	51
Figure 32: Ductile failure of CT sample.....	52
Figure 33: Dissipated energy of AT oriented CT samples.	53
Figure 34: Dissipated energy of TT oriented CT samples.....	53
Figure 35: Dissipated energy of TA oriented CT samples.	54
Figure 36: Displacement-load graph of three failure modes.	54
Figure 37: Corrected load/displacement curves of uncompressed SENB samples aged at 105°C. Combined data from Strabala [1] & Meagher.	61
Figure 38: Corrected load/displacement curves of 25% compressed, TT oriented SENB samples aged at 105°C. Combined data from Strabala [1] & Meagher.....	61
Figure 39: Corrected load/displacement curves of 25% compressed, TA oriented SENB samples aged at 105°C. Combined data from Strabala [1] & Meagher.....	62
Figure 40: Corrected load/displacement curves of 50% compressed, TT oriented SENB samples aged at 105°C. Combined data from Strabala [1] & Meagher.....	62

Figure 41: Corrected load/displacement curves of 50% compressed, TA oriented SENB samples aged at 105°C. Combined data from Strabala [1] & Meagher.....	63
Figure 42: Corrected load/displacement curves of unaged SENB samples. Combined data from Strabala [1].	63
Figure 43: Corrected load/displacement curves of uncompressed, AT oriented CT samples, aged at 125°C.....	64
Figure 44: Corrected load/displacement curves of 15% compressed, AT oriented CT samples, aged at 125°C.....	64
Figure 45: Corrected load/displacement curves of 25% compressed, AT oriented CT samples, aged at 125°C.....	65
Figure 46: Corrected load/displacement curves of 35% compressed, AT oriented CT samples, aged at 125°C.....	65
Figure 47: Corrected load/displacement curves of uncompressed, TT oriented CT samples, aged at 125°C.....	66
Figure 48: Corrected load/displacement curves of 15% compressed, TT oriented CT samples, aged at 125°C.....	66
Figure 49: Corrected load/displacement curves of 25% compressed, TT oriented CT samples, aged at 125°C.....	67
Figure 50: Corrected load/displacement curves of 35% compressed, TT oriented CT samples, aged at 125°C.....	67
Figure 51: Corrected load/displacement curves of uncompressed, TA oriented CT samples, aged at 125°C.....	68
Figure 52: Corrected load/displacement curves of 15% compressed, TA oriented CT samples, aged at 125°C.....	68
Figure 53: Corrected load/displacement curves of 25% compressed, TA oriented CT samples, aged at 125°C.....	69
Figure 54: Corrected load/displacement curves of 35% compressed, TA oriented CT samples, aged at 125°C.....	69

Chapter 1. Introduction

Glassy polymers such as polycarbonate (PC) can be toughened through compressive plastic deformation. The increase in toughness is substantial; as much as a fifteen fold increase in the amount of dissipated energy during failure. This toughness increase can likewise be reversed through thermal aging at high temperatures below the glass transition temperature (T_g). In this thesis, the combined effects of plastic compression and thermal aging have been studied. After physical aging, the PC transitions from its toughened state to a brittle state similar to that of PC that has not been compressed. This transition from a toughened state to a brittle one can be abrupt with a region of bimodal behavior in which the samples behave either like a toughened sample or brittle uncompressed sample. This aging time needed to force a transition from a toughened state can be different depending on the amount of plastic compression and the orientation of the sample.

In this chapter, an introduction of polycarbonate will be given along with an outline of the previous research that has been conducted on this subject and the experiments performed. Following this, an outline of the sample preparation and the procedure and results of each set of experiments is given.

1.1 Polycarbonate

The production of Polycarbonate (PC) is one of the largest of the glassy polymers. One of the main reasons for this growth is the ideal properties of this polymer, characterized by its high modulus and toughness. PC is most commonly processed from bisphenol A and phosgene to yield the monomer seen in Figure 1. [2]

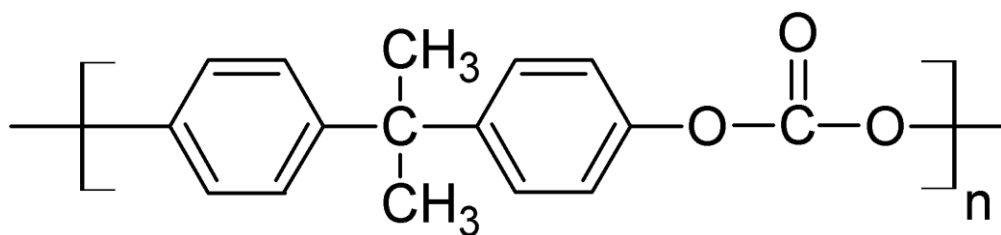


Figure 1: PC monomer [2].

This particular monomer most notably contains a carbonate group, (O-(C=O)-O), the source of the polymer's name, connected to two benzene rings separated by a propyl group. It can be seen in this structure that there is a limited amount of flexibility given the benzene rings and the double bond on the carbonate group that is indicative of the stiffness. Furthermore the strong covalent C-O and C-C bonds are indicative of high strength.

As PC is a glassy polymer, the material undergoes a key morphological change after the temperature drops below the glass transition temperature (T_g), $\sim 147^\circ\text{C}$. While the material is above this temperature, the polymer chains have a significant freedom of motion and are able to flow easily, and the material is considered to be in a rubbery state. Once the temperature drops below this point, the polymer chains freeze into place. If this process is gradual and the temperature drops slowly the chains will be closer to an

equilibrium state than if the material is quickly cooled or quenched. In this case the chains are locked into place, creating areas of internal stress between opposing polymer chains. Yet, when the material is below the glass transition, the polymer chains can still be displaced relative to each other through mechanical loading by applying large forces. When the PC is deformed, the polymer chains will be strained and will begin to orient themselves. This behavior is shown, in an exaggerated manner, in Figure 2. All of these morphology changes induced below the glass transition can be reversed by raising the temperature above the glass transition.

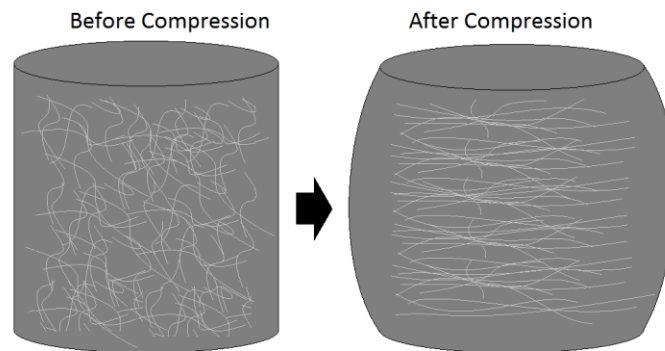


Figure 2: Exaggerated change in orientation of PC polymer chains

The properties of high strength and stiffness observed in PC make it ideal for high performance applications, such as using as a key component of ballistic glass, protective visors, aircraft canopies, or any application which requires a tough transparent material that will protect someone or something from impacts and outside forces while giving the best clarity to view outside objects.

Because polycarbonate is a key component of many high performance applications, it is necessary to understand how PC reacts and changes over time when

exposed to high temperatures, UV radiation and other elements. These are all various forms of what is known as aging. In this work the focus is on thermal aging which is essentially heating to a high temperature below the glass transition temperature (T_g) and holding for an extended periods of time. While it is important to understand how this material reacts over time, it is just as important to determine how one can improve this material. That is, make it stronger, tougher, and more resistant to aging.

As with most glassy polymers, PC can be further toughened through plastic deformation [1, 3-15]. This has been specifically observed in Izod impact tests performed by Thakkar, et al. [3]. Physical aging is known to change the properties of glassy polymers [14-29], specifically make them more brittle. Additionally, the effect on relaxation that that might be responsible for removing the toughened state of deformed PC has been shown by Thakkar, et al. [14] & Ho, et al. [25] who observed the relaxation of polymer chains leading to a transition from a ductile to brittle failure mode with thermal aging. Additionally, Ho and Vu-Khanh observed that a greater internal change occurred at higher temperatures [23]. Because of this known behavior the goal of this research was to combine these two behaviors at higher compressions and see if aging could affect the positive increase in toughness induced by plastic compression.

In addition to the increased toughness induced from plastic deformation, the deformed PC becomes mechanically anisotropic along different orientations [1,3-5]. This is seen, for example, in the ultrasonic anisotropic wave speeds measured along different orientations with respect to the axis of compression of PC samples, as shown in Figure 3.

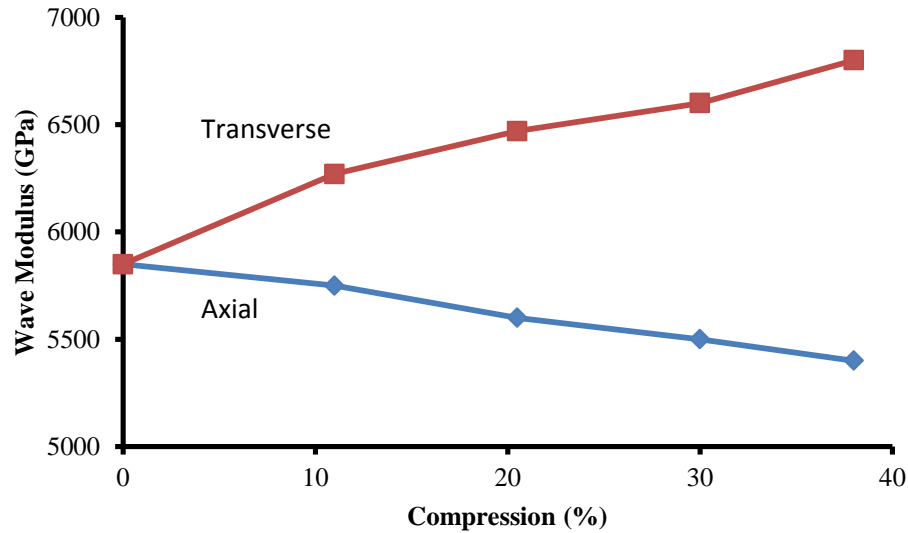


Figure 3: Anisotropy of ultrasonic wave modulus measured in plastically compressed PC Samples [5].

However, the research that studies the anisotropy is very minimal. As will be shown, the anisotropic behavior is very pronounced and might, therefore, be important. This is not only in terms of characterizing the fracture behavior, but also might provide key information in understanding the internal structural mechanism that causes the toughening of PC after plastic deformation.

1.2 Previous Work

As was mentioned earlier, many studies have performed fracture experiments on compressed and or aged polycarbonate, such as the articles by Thakkar et al. [3, 14] and Ho & Vu-Khanh [25]. The scope of the experiments conducted in these works was much smaller than the current study. Fewer samples were tested and the studies did not deal with samples that had been deformed to the extent done here. Furthermore, many of the conclusions that were made by Thakkar regarding the toughening mechanism were

incomplete. It had been observed that in samples that displayed tougher fracture behavior there were internal stresses measured through the layer removal technique [3] present that were not present in uncompressed samples or samples that had lost their toughness after thermal aging. These internal stresses were believed to be the cause of the increase in toughness. While there is a correlation between the increase in toughness and the internal stresses, the stresses are not the cause of the toughness increase as was indicated by Oh & Kim[6].

It was shown by Oh & Kim [6] that an increase in toughness is not due to the internal stresses but instead may be attributed to a morphological change of the material through rolling compression. The results of this thesis strongly suggest that the increase in toughness is attributed to the morphological change of material, specifically the orienting of polymer chains as a result of the plastic deformation.

The concept of anisotropic behavior in the compressed polycarbonate is seen in the longitudinal wave speed measurements performed by Goel, et al. [5], which showed an increasing difference, as a function of compression, in the ultrasonic moduli measured along the axis of compression (axial) and perpendicular to the axis of compression (transverse). This anisotropy in the wave speed suggests a change in the internal structure of the PC after compression. This changing of the morphology, which would be the displacement and orienting of the polymer chains would cause the resulting change in internal stresses that were observed by Thakkar, et al. [3,14], which were not the cause of the change in the PC but merely a correlation with the change.

As the topic of this thesis is a continuation and expansion of the fracture tests performed by Strabala [1], it is important to look at what was done and what was

concluded from the fracture tests. A total of 96 Charpy Impact and 48 quasi-static Single Edge Notched Bending Tests were performed on uncompressed and compressed samples (25% and 50% strain) without aging and with aging at 125°C for 20, 50, 100 and 300 hours and.

His results showed an anisotropic increase in toughness of the PC samples that was dependent on the orientation of the crack propagation direction with respect to the direction of compression. As the compression increased, the difference in toughness in the two orientations became larger as well. The anisotropy was also seen in the amount of aging time required for samples of different orientations to become brittle again. The samples whose orientation was weaker transitioned from a toughened state before the sample from the tougher orientation. Additionally, the Charpy samples compressed to 50% strain did not undergo a transition from their toughened state after all aging times (up to 300 hours). These results were valuable in introducing the behavior of such highly compressed samples, but there was not enough data to be conclusive. Thus he called for further experiments to be performed to confirm his initial conclusions and to fully characterize the effects of temperature, aging time, and orientation on this change.

1.3 Tests Performed

Three sets of mechanical fracture experiments were performed. The first set was Charpy Impact tests. These were performed to measure the fracture behavior of the material under dynamic loading conditions. The other two sets of experiments were a pair of quasi-static fracture tests performed on samples of two different shapes. These shapes were the shape used Single Edged Notched Bending (SENB) tests and one developed for Compact Tension (CT) tests. The reason for the introduction of the CT

samples was due to the size restrictions of the compressed PC cylinders, which were not large enough to make SENB samples along all three orientations.

The Charpy and SENB tests performed were supplementary to the Charpy and SENB tests performed previously by Strabala [1]. As Charpy and SENB tests had been performed on samples aged at 125°C, a second batch of Charpy and SENB tests were performed on samples aged at 105°C for longer aging times to compensate for the lower temperatures. These times were 300, 700, 1500, 3000 and 6000 hours. Additional Charpy tests were performed to study the effect of aging temperature on the rate at which compressed PC transitions from toughened to brittle failure. Additional SENB tests were performed to add data points for aging times where large uncertainty was present in the initial data.

The CT samples were a new set of experiments performed on samples that had been previously annealed and quenched before compression. These samples were aged at 125°C for 20, 50, 100, 300 hours. The same orientations as those studied in the Charpy and SENB tests were studied in the CT tests along with a third orientation that was not possible to make from the compressed bars used for the other tests.

In total, 343 fracture tests were performed (142 Charpy, 81 SENB, and 120 CT) in addition to the 144 fracture tests (96 Charpy & 48 SENB) performed previously by Strabala [1], for a combined total of 487 fracture tests.

Chapter 2. Sample Preparation

The Charpy and SENB samples were sourced from large GE Lexan 9034 sheets (8' x 4' x ½"). The CT samples were sourced from 1" diameter PC rods from Sabic Innovative Plastics under the name Natural PC.

2.1 Pretreatment

The Charpy and SENB samples were prepared from PC that did not undergo any thermal treatment before being plastically compressed. This differed from the PC used for the CT samples which were annealed and quenched. The procedure for this process is as follows:

1. Hold samples at 105°C for 3 days, to remove any water present inside the PC
2. Anneal at 150°C for 2 hours, to remove thermal history.
3. Water quench in room temperature water, ~23°C, after removing from 150°C oven.

The intent of this process, as outlined by Strabala [1] was to remove any thermal history in the PC rods. But, as outlined by Thakkar, et al. [14], while this sort of annealing does remove the previous thermal history, the fast quenching in water actually

introduces a new set of internal stresses to the PC by quickly freezing the polymer chains and not allowing them to settle closer to equilibrium configuration. It was this documented change of the internal structure of PC under these treatment conditions that motivated the testing of CT samples to compare with the Charpy and SENB tests.

2.2 Compression

Charpy and SENB samples were performed on uncompressed PC and PC plastically compressed to 25% and 50%. This compression was performed on 80 mm x 12.7 mm x 50.8 mm bars cut from the PC sheets. These bars were compressed to a plastic engineering strain of either 25% or 50% with a 20,000 kN load frame. During compression, a Teflon lubricant was used to minimize the risk of any unwanted deformation such as cracking or shearing of the material. Two plastically compressed bars and one uncompressed plate are shown below in Figure 4.

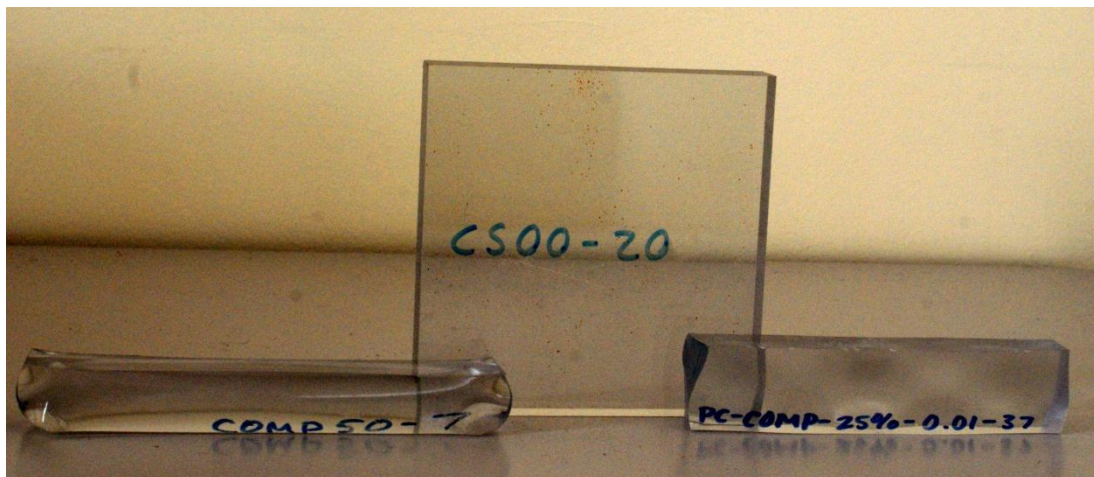


Figure 4: Uncompressed PC sheets & 50% (left) & 25% (right) compressed PC bars used to prepare Charpy & SENB samples

The cylinders used to make CT samples were compressed using the same 20,000 kN load frame. Samples were compressed to 15%, 25% and 35% engineering strain, each with a final height of around 27mm. Again, a Teflon lubricant was used to minimize the risk of unwanted damage. The compressed samples are shown below in Figure 5.



Figure 5: Compressed PC cylinders used to prepare CT samples, from left to right: 0%, 15%, 25%, 35% & 40% compression.

2.3 Thermal Aging

Thermal aging was performed on all samples in isothermal ovens, monitored by electronic thermocouples.

2.4 Sample Machining

Charpy and SENB samples were closely related to each other in that their dimensions were the same; with only the notch style differing between the two. Samples were cut and machined from the compressed and uncompressed bars to final dimensions of 10 mm x 4 mm x 80 mm using a 25 mm endmill at 800 rpm. A liquid coolant/lubricant was used during all stages of cutting and milling so as to not affect the

polycarbonate through overheating. Machining to final dimensions was always performed after physical aging, as samples would tend to warp slightly after long periods of aging.

The notching of the Charpy and SENB samples was what differentiated the two. The Charpy samples underwent a much simpler notching process. After machining to final dimensions, a 2 mm, 45° impact notch was cut so the sample width was reduced from 10 mm to a uniform 8 mm for all samples. The notch was made with a hand-cranked Charpy sample notching machine (CEAST 6816). The maximum thickness of each cut by the crank was 0.2 mm; the final 0.2 mm of each notch was done by removing 0.05 mm on each cut. This diagram is pictured below in Figure 6.

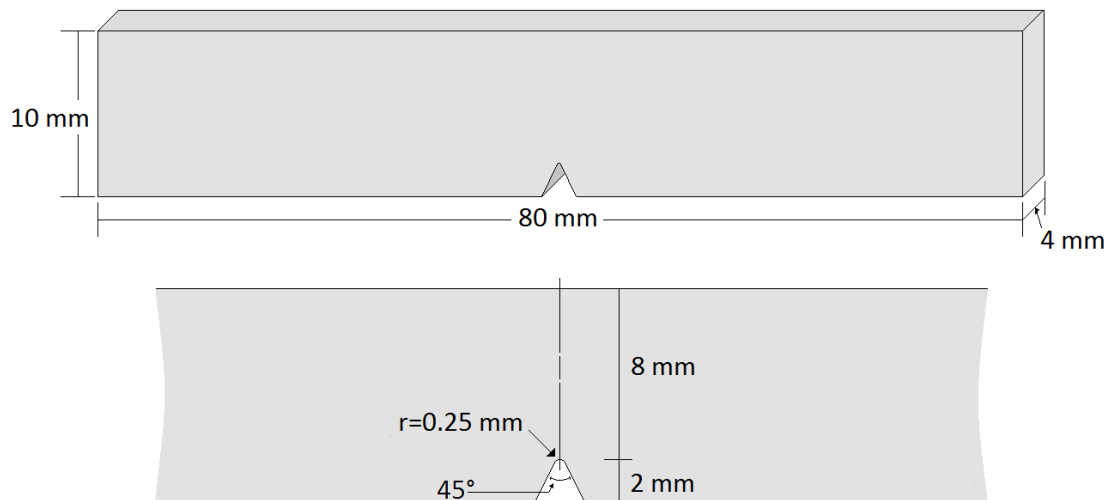


Figure 6: Charpy sample geometry & notch diagram

The SENB Samples had a more complicated notch. After machining to final dimensions, a 4 mm, 45° notch was cut using the same hand-cranked Charpy sample notching machine. A set of teeth, machined at 45° in opposite, were then machined into the sample. These teeth were machined using a 2 mm endmill. The purpose of these teeth was to accommodate the use of an extensometer to measure the Crack Tip Opening Displacement (CTOD). Finally a 1 mm crack was then created at the base of the notch by tapping a razor blade with a hammer. The final width between the notch tip and the back of the sample was 5 mm. The diagram of the SENB sample geometry and notch is shown below in Figure 7.

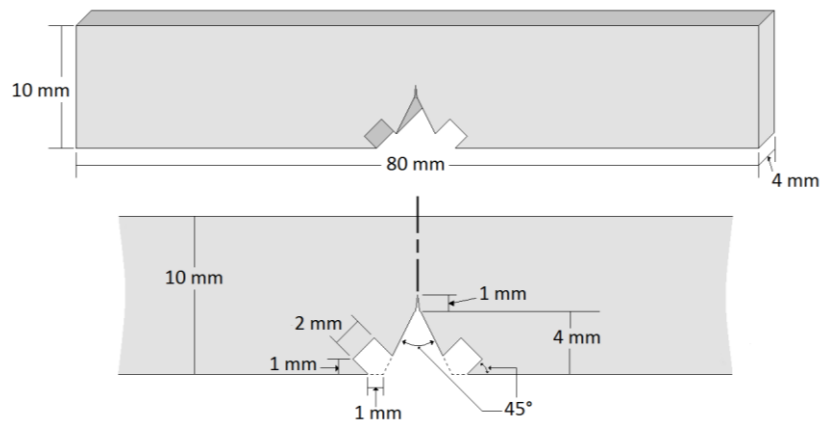


Figure 7: SENB sample geometry & notch diagram

The Charpy and SENB samples were cut in two orientations. Samples were cut such that their long axis was perpendicular to the axis of compression, and their widths were either along the axis of compression or perpendicular to this axis. As a result, the samples had a long axis that was transverse to the axis of compression and the notches

would induce fractures that ran along the axis of compression, or transverse (perpendicular) to it. These samples were designated as TA and TT, where the first letter indicates the direction of the length of the sample (transverse to the compression axis in both cases) and the second letter indicates the direction of the width, which is also the direction of the crack propagation. The TT samples had their notches pointing transverse to the axis of plastic compression and the TA samples had their notches pointing along the axis of plastic compression. This difference in orientation can be seen in Figure 8.

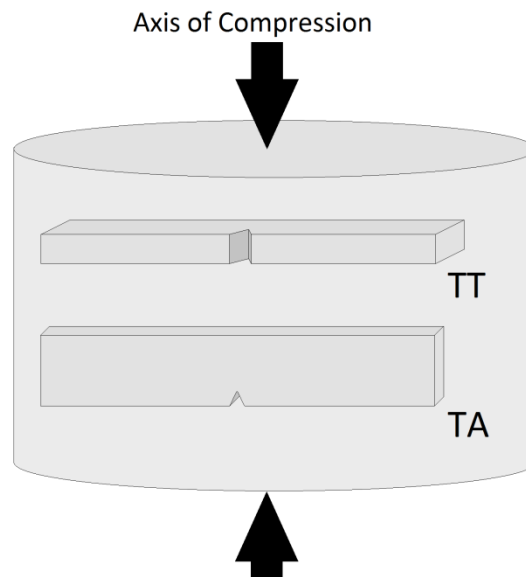


Figure 8: TA & TT sample orientations for Charpy & SENB samples.

CT samples were cut and machined to final dimensions of 18 mm x 18 mm x 7 mm. This size was chosen as it was the largest dimension that could be prepared from cylinders of all compressions (0%-35%). As machining the cylinders is awkward, the cylinders were cut in half, either along the axis of compression or perpendicular to it, using a ceramic cutting wheel. Like the Charpy and SENB samples, CT samples were

machined using a 25 mm endmill at 800 rpm. Just as was done in the preparation of early samples, liquid coolant/lubrication was used so as not to affect the PC by overheating.

After the CT samples had been machined to their final dimensions, the samples were drilled and notched. Before the samples were notched, they first needed to have mounting holes drilled so that displacement correction measurements could be taken. These mounting holes were made with a vertical drill press using a 2.75 mm diameter drill bit. The diameter nearest to the mounting pins used in the apparatus. After correction measurements were performed, a 9 mm notch was machined with a 2 mm endmill at 800 rpm. A 2 mm crack was then created at the base of the machined notch with a razor blade in the same manner as the SENB samples as shown in Figure 10. The total remaining width was 7.2 mm as shown in Figure 9.

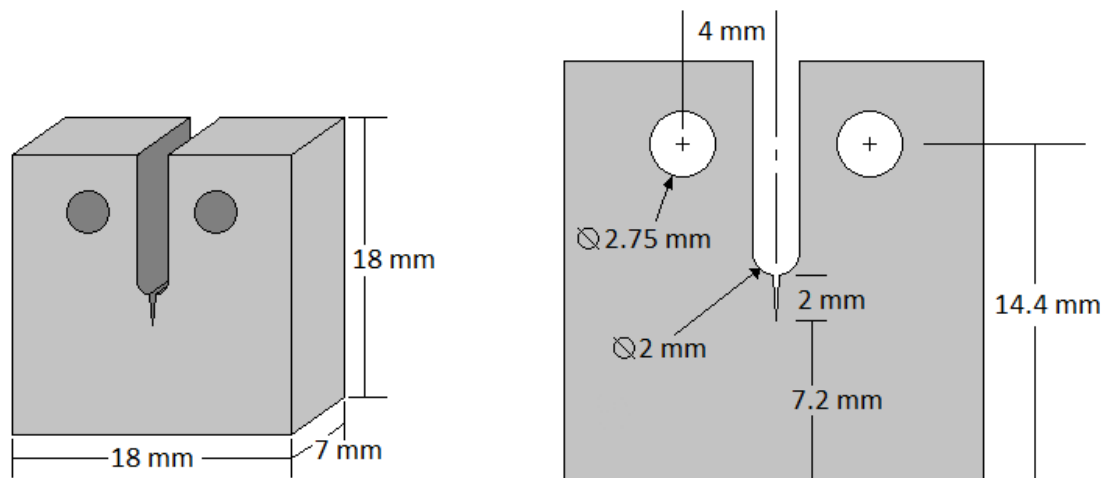


Figure 9: CT sample geometry & notch diagram.



Figure 10: Crack notching of CT sample with a razor blade.

Like the Charpy and SENB samples, the CT samples were cut in various orientations to study the anisotropic behavior as a function of compression. Due to the size of the samples, we were able to get samples in three orientations so we had TA, TT, and AT samples. Just like the Charpy and SENB samples, the notation for CT samples remains the same.

The three orientations used for the CT samples were AT, TT and TA. The AT and TT samples allowed the comparison of samples whose cracks propagated in the same direction with respect to the axis of compression, transversely, but were cut in different orientations. The TA samples, differed from the other two orientations as their crack propagated along the axis of compression. The difference of the three orientations can be seen below in Figure 11.

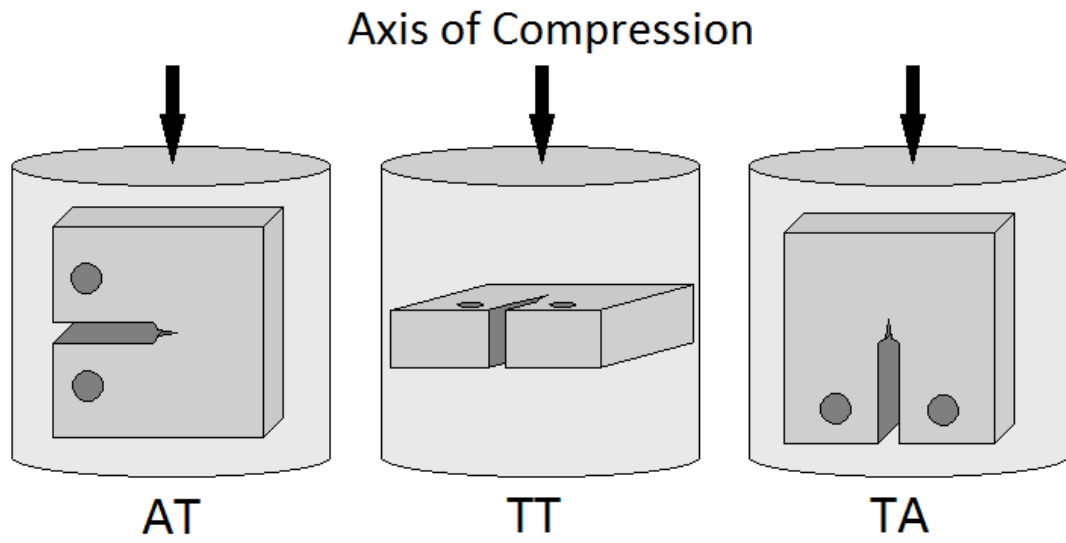


Figure 11: AT, TT and TA Orientations of CT Samples

Chapter 3. Charpy Impact Tests

3.1 Introduction

As one of the key applications of PC is in dynamic impact protection, e.g. ballistic glass, protective eyewear, it is extremely important to study and characterize the behavior under dynamic impact tests. Charpy impact tests were used for this reason. These tests were performed to supplement the tests performed by Strabala [1], and were conducted on samples aged at different aging times and/or temperatures. Samples were prepared and tested according to the methods used by Strabala [1].

3.2 Procedure

Polycarbonate (GE Lexan 9034) was used for the Charpy impact samples. Samples were machined from uncompressed and compressed bars both cut from larger 8' x 4' x 1/2" PC sheets. The compressed bars were compressed to a final plastic strain of 25% and 50%. Sample sets were thermally aged for specific times at temperatures between 105 °C and 135 °C. The aging temperatures were below the glass transition temperature of PC, which is 147 °C.

Samples were machined to the final dimensions of 10 mm x 4 mm x 80 mm in the TA and TT orientations. After machining to final dimensions, a 2 mm, 45° impact notch was cut so the sample width was reduced from 10 mm to a uniform 8 mm for all samples.

The notch was made with a hand-cranked Charpy sample notching machine (CEAST 6816).

Charpy tests were performed on a Charpy impact machine (CEAST 6545) using a 15J hammer. The distance between supports was 40mm with the hammer impacting the sample directly between the supports. The energy dissipated by the samples during the impact and fracture was measured by the difference in potential energy of the pendulum before and after the test. This measurement was performed electronically by the Charpy machine by measuring the difference in the height of the pendulum between the beginning and end of the swing. The energy lost to friction was recorded by measuring the energy loss when no impact occurred. This value, 0.03J recorded at all instances, was subtracted from the recorded dissipated energy of each sample during data analysis. Additionally, before tests were performed a couple of dummy samples would be broken to warm up the Charpy impact machine, as was done by Strabala [1]. Figures 12 and 13 show the Charpy impact tester.



Figure 12: Charpy Testing Machine (CEAST 6545)



Figure 13: Charpy Sample Mount & Impact Hammer

The initial Charpy tests were performed over a broad range of aging times at 105 °C and at 125 °C to provide a baseline of the behavior for the compressed and aged

samples. Follow up tests were performed at various other temperatures ranging from 115 °C to 135 °C to establish the temperature dependence of the ductile to brittle transition observed in the initial tests. Additional tests were also performed in the transition zones to better characterize this range.

Charpy tests were conducted for undeformed samples and samples compressed to 25% and 50% plastic strains. Undeformed and plastically deformed samples were thermally aged at both 105°C and 125°C. The aging at 105°C was done for up to 6000 hours and the aging at 125°C was done for up to 600 hours. At least 3 samples were tested at each plastic deformation and aging time at 125°C and at least 2 samples at each plastic deformation and aging time at 105°C. After identifying the ranges for aging that resulted in a drop in the Charpy result, up to 7 additional Charpy tests were done for aging times in the transition regions for the 25% compressed samples, and a number of new aging times were added to better define the transition.

The effect of temperature on the drop in Charpy results with aging in the 25% plastically compressed samples were studied by conducting additional aging tests at 120°C, 130°C, and 135°C. In each case, at least 4 samples were aged and tested at each aging temperature and each aging time.

3.3 Results

The failure in the samples could be categorized into three different modes as shown in Figure 14-16. These included brittle fracture, ductile fracture, and mixed fracture, characterized by crazing. The samples failing by brittle fracture all split into two parts and the surface of the fracture was smooth as indicated in the picture. The samples undergoing ductile fracture bent into a “V” shape but stayed intact, simply bending

enough to allow the hammer to pull them through the space between the two sides of the holder. The surface of these samples was rough and the sample showed substantial deformation around the failure region. The samples in the third category split into two, but had a rough surface.

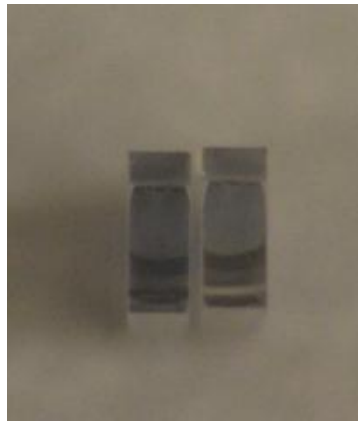


Figure 14: Fracture Surface of Brittle Samples



Figure 15: Fracture Surface of Samples with Mixed Mode Failure (Shearing & Tensile Failure)



Figure 16: Fracture Surface of Ductile Samples

At 125°C the samples failed in all three modes. The undeformed samples showed a brittle failure for all aging times. At 25% plastic compression, the TA samples showed ductile failure, but transitioned into brittle failure with the increase of aging. At 50% plastic deformation, the TA samples showed ductile failure for all aging times without showing any change of failure mode for all the aging times. The TT samples initially showed a mixed failure mode, showing characteristics of both the brittle and ductile failure. At 25% compression, the TT samples first failed in a ductile mode, but with aging transitioned into a classical brittle fracture. At 50% compression, the TT samples showed a mixed mode in which the samples fully broke, but the surfaces were rough showing substantial plastic flow on the fracture surface. Similar results were seen at 105°C.

Figures 17 and 18 show the dissipated energy obtained from the Charpy tests conducted on samples aged at 105°C and 125°C respectively. The Figures show the results from Charpy tests on PC for uncompressed, plastically compressed to 25% and plastically compressed to 50%. Figure 17 shows the results for 105°C aging temperature and Figure 18 shows this for 125°C. Each data point indicates the average of a number of Charpy tests conducted for the given plastic strain, aging temperature and aging time.

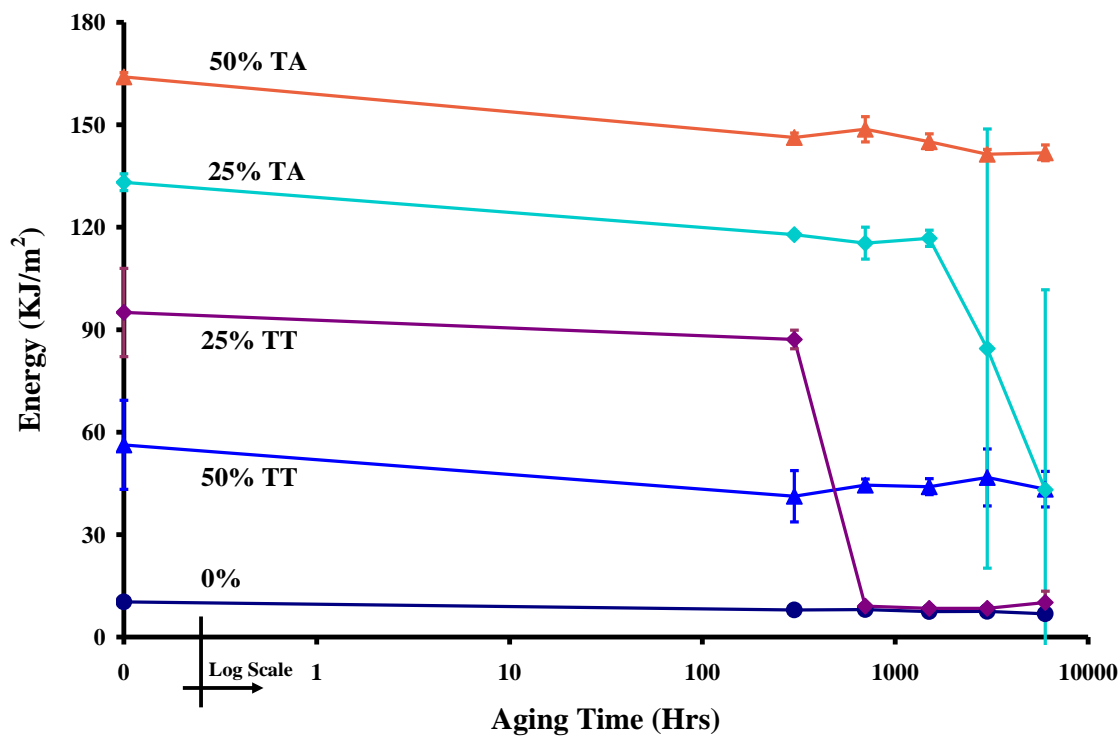


Figure 17: Energy dissipation of Charpy samples aged at 105°C. Combined data from Strabala [1] and Meagher.

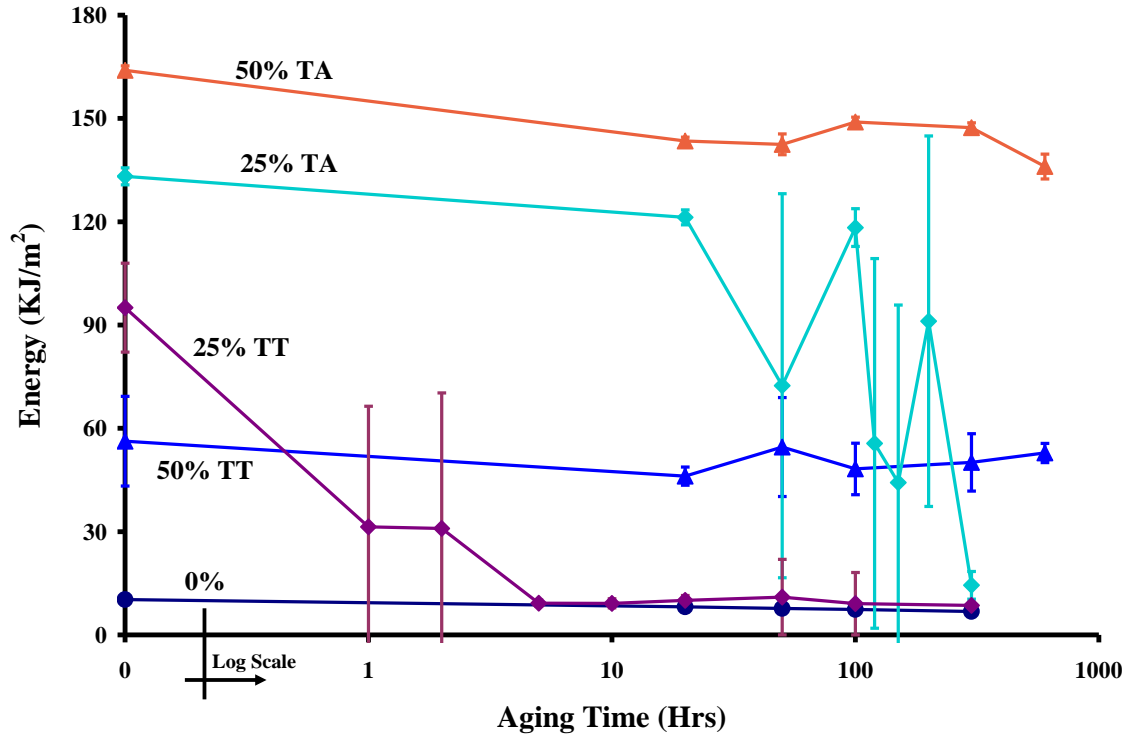


Figure 18: Energy dissipation of Charpy samples Aged at 125°C. Combined data from Strabala [1] and Meagher.

As can be seen, the undeformed samples show a low dissipated energy which drops slightly with aging at the given temperatures. On the other hand, both the TA and TT samples indicated a higher energy after subjecting the material to plastic strain, and this energy was higher in the TA samples when compared to the TT samples. The 25% compressed samples showed a substantial drop of the measured dissipated energy after aging, while the 50% plastically compressed samples did not show substantial change in this range of aging temperatures and times.

Figure 17 shows the energy loss measured in the Charpy test for samples aged at 105 °C for times up to 6000 hours. In the case of the samples compressed to 50%, there was no change in the fracture mechanism for either TA or TT samples, regardless of aging time. The initial energy dissipation increases for the 50% TA samples were

significant. For these samples we measured an energy dissipation of 164 KJ/m^2 compared with 10 KJ/m^2 energy dissipation for uncompressed samples. This indicates an initial improvement of approximately 16 times over the undeformed sample. This energy dissipation dropped to about $140\text{-}151 \text{ KJ/m}^2$ with aging. In the case of the 50% TT samples the initial increase in dissipated energy was less pronounced but still significant. We measured an initial energy dissipation of 56 KJ/m^2 . After aging this value was approximately $36\text{-}52 \text{ KJ/m}^2$.

The Charpy tests performed on 50% compressed samples that were aged at $125 \text{ }^\circ\text{C}$ showed the same behavior as described for the $105 \text{ }^\circ\text{C}$ aged samples, essentially retaining most of the increase in dissipated energy even after aging.

In the case of the 25% compressed samples the initial increase in the energy dissipated was less pronounced when comparing the 25% compressed TA sample to the 50% compressed TA sample, but more pronounced when comparing the TT samples. The initial energy absorbed by the TA sample was 133 KJ/m^2 , and for the TT sample it was 95 KJ/m^2 , indicating a factor of 10 to 13 increase in dissipated energy when comparing to the undeformed sample depending on the orientation of the impact.

After aging, the 25% compression samples underwent a transition from their elevated energy dissipation to a much lower energy dissipation, roughly reaching the response of the uncompressed samples. In this sense the samples seemed to lose all the benefits of plastic working when sufficiently aged. An interesting feature in this change was that the aging time associated with the drop in properties was different for the TA and TT samples. For example, for the case of aging at $105 \text{ }^\circ\text{C}$, the transition for the TT occurred between 300 and 700 hours, while the transition for the TA samples occurred

For the 25% TA samples aged at 125 °C there was a broad aging time range from 20 hours of aging where all the samples underwent a ductile failure to 300 hours when all samples underwent brittle failure. Between the two aging times the samples either underwent one or the other mode failure. To further study the transition, we selected five times between these limits and did seven tests at each aging time in this transition zone. As can be seen in Figure 19, in the transition the samples showed energy dissipation which was either that associated with the high energy seen in the ductile failure before the start of the transition time or they showed the low energy failure seen after the end of the transition zone. The number of failures associated with each mode was fairly random in the transition zone, even though one might expect better control over the experiment might indicate a statistical distribution that shows a bias to one failure mode at the start of the transition and the other at the end. This same bimodal and random characteristic was seen in the failure modes when examining the failure surfaces.

A similar characteristic was seen in the TT samples at 25% plastic compression and aged at 125°C shown in Figure 20. Even though the start failure mode was different and the energy level was different. Similar results were also seen for the 25% plastically compressed TA and TT samples at 105°C.

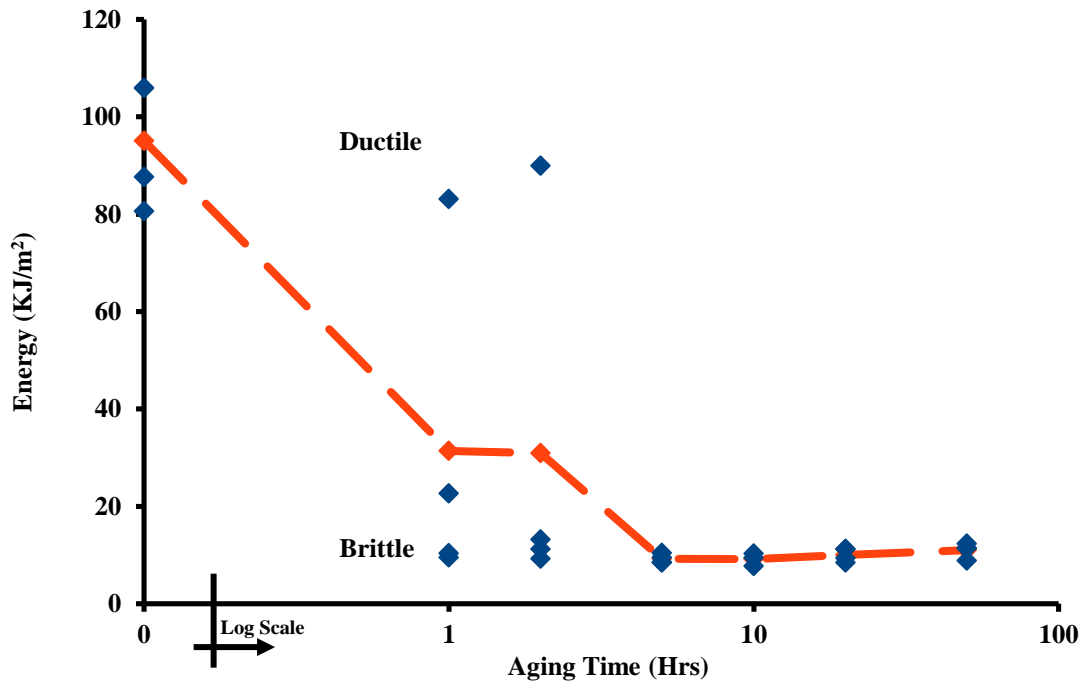


Figure 20: Energy dissipation of individual Charpy samples in the transition zone (25% TT, 125°C aging). Combined Data from Strabala [1] and Meagher.

To study the effect of temperature on the transition observed in the 105°C and 125°C aged samples, a series of experiments were performed on 25% TA samples at various aging times and temperatures. Figure 21 shows the result of this study for aging at temperatures between 105°C to 135°C. The figure plots the aging time as a function of aging temperature and indicates the nature of the failure. As can be seen, this preliminary study indicates that the transition zone shrinks and occurs at smaller aging times as we move to higher aging temperatures. The number of data points is not sufficient to clearly identify the transitions, yet suggests that the drop could happen much sooner with aging at higher temperatures, essentially totally losing the benefits of plastic working, possibly even for the large plastic compressions.

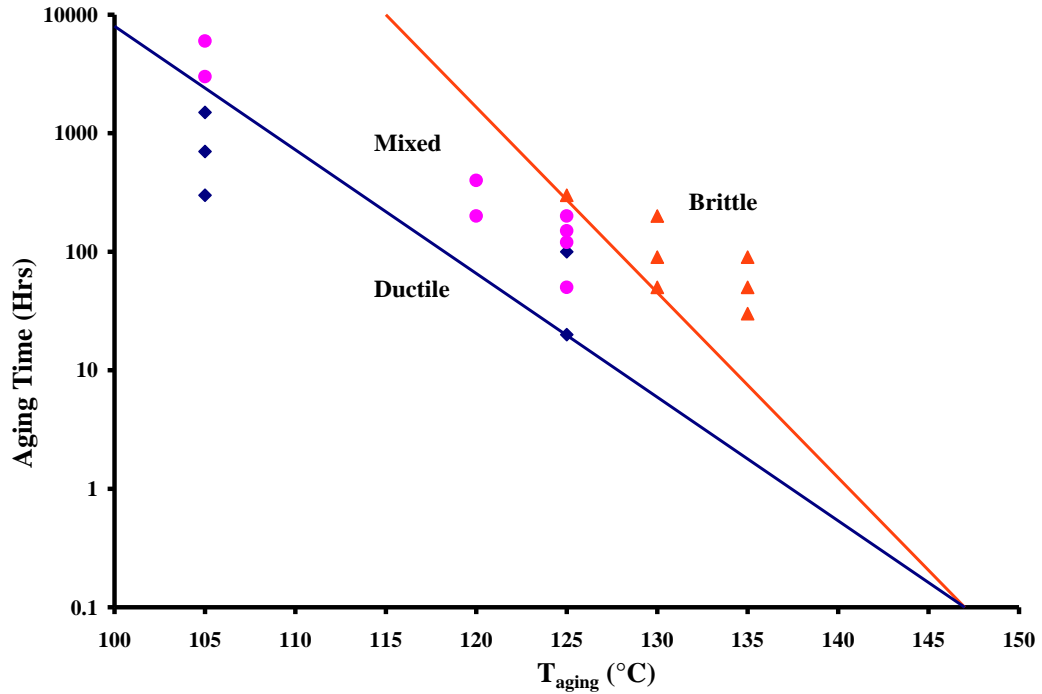


Figure 21: Failure mode of Charpy tests as a function of aging time and temperature.

3.4 Discussion

In both compressions (25% & 50%) and orientations (TA and TT) a significant increase in energy dissipation occurred after compressive plastic flow. The greatest increase in energy dissipation occurred in TA samples for both 25% and 50% compressions. For the TA samples the increase in energy dissipation for the two compressions was thirteen and sixteen times greater than the uncompressed samples. In the case of the TT samples compressed to 25% and 50% compressions, the increase in energy dissipation was less pronounced, but still significant. In the TT samples this increase was, respectively, nine and six times greater than uncompressed samples.

Initially, all of the compressed samples, with the exception of the 50% TT samples, broke in a ductile manner as opposed to the uncompressed samples which broke in a brittle manner, though with significant roughness at the fracture surface. As noted earlier, the fracture surfaces of the 25% TT samples contained crazing marks as opposed to the smooth surfaces of the TA samples for both compressions. These failure modes are important to note as they indicate the type of stress that caused the fracture in each of the samples. As ductile tearing is indicative of shearing and brittle fracture indicates tensile failure, it can be understood that the uncompressed samples were able to fail due to weak tensile resistance. On the other hand the TA samples, both 25% and 50% compressed, were more resistant to tensile stresses, thus failing through shear tearing. Finally the TT samples failed in the mixed mode where a combination of tensile and shear stresses contributed. This indicates an increased resistance to tensile stresses over the uncompressed samples, though inferior to that of the TA oriented samples.

With the addition of aging at temperatures below the glass transition temperature, the samples showed a loss of all or part of the toughness gained from the compression. The time it took to lose the additional energy was dependent upon both the amount of plastic compression and the orientation of the Charpy sample relative to the axis of compression. In the case of the 25% TT samples, the loss of toughness happened very quickly when aged at 125 °C. In this case, at both aging times of 1 and 2 hours we had 3 out of 4 samples break with the same dissipated energy as an uncompressed sample, such that none of the observed benefits of compression were apparent after even such a short aging time for most samples. After 5 hours of aging, all samples for this case broke with the same dissipated energy as the uncompressed samples. For 25% TA samples, the

transition from tough/ductile to weak/brittle failure occurred much later, at 50 hours aging at 125 °C. This difference in transition times affirms a distinct anisotropic behavior of the ductile to brittle transition dependent on the orientation of the sample, this same difference in transition occurs in the samples aged at 105 °C, but at a delayed time due to the lower aging temperature.

For 50% plastically compressed samples, there was no significant transition from the tougher states that was found at any aging time at either 105 °C or 125 °C. In the case of 50% TA samples, there was a drop in energy dissipation of roughly 10% after the first aging interval at 125 °C (20 hours) and 105 °C (300 hours) and after this initial drop the energy dissipation stayed relatively constant. Figure 21 indicates that higher aging temperatures might move the transitions to shorter times suggesting that further study at these higher aging times and temperatures might of the 50% compressed samples produce observable transitions.

In addition to the anisotropic behavior of the ductile to brittle transition, there was also a distinct anisotropy that occurred as a result of plastic compression. In Figures 17 and 18, it can be seen that the difference between the two orientations (TA and TT), for unaged samples, is much greater at 50%. Specifically in the case of the 50% samples, this anisotropy was made more evident in the difference in fracture modes as seen in Figures 14, 15 and 16. For the TT samples a quasi-brittle mode occurred in that there was a full break of the sample but with localized striations appearing on the fracture surface causing energy absorption greater than a simple with brittle fracture. On the other hand, the TA samples displayed the tougher ductile breaking resulting in a sample that

never fully broke. This difference of fracture modes occurred at all aging times and temperatures tested.

What is the cause of this anisotropic behavior in the ductile to brittle transition? It was concluded in previous work that the internal stresses present in PC samples that have been plastically deformed are the cause of the toughening in polycarbonate [3]. So would then be logical to think that the internal stresses affecting the TT orientation would be fewer, resulting in both the lower energy dissipation during impact and a quicker transition from ductile or toughened state to the original brittle state due to fewer stresses being relaxed at the high temperature aging. However when the results from the 50% plastically compressed samples are considered, this logic does not apply.

Instead it should be considered that these internal stresses are not the cause of the toughness but instead are simply evidence of the structural mechanism that is causing the increased toughness. The internal stresses should instead be considered a byproduct of the plastic flow of polymer chains that rearrange and become more perpendicular in relation to the axis of compression as deformation increases. And this rearrangement would require that the fractures running along the axis of compression, such as those in TA samples, would have to break more polymer chains per unit length than would be expected for fracture in the TT samples.

Additionally, it has been observed that the induced toughness is relaxed by high temperature, sub- T_g aging [14, 17]. This relaxation of the polymer chains in PC that has been observed both in previous literature and in this work would support the proposed mechanism of toughening through increased polymer chain orientation. As the oriented

polymer chains relax and become less oriented, they would allow the material to transition back to the brittle fracture mode.

It was discussed earlier that between 105 °C and 125 °C aging, there was a clear shift in the time of the transition for all the 25% samples, both TA and TT. A small sample set was taken to explore this change in transition time as a function of aging temperature at various temperatures ranging from 115 °C to 135 °C. The aging times were chosen so as to match along an exponential curve fit between the times of corresponding fracture modes of the 105 °C and 125 °C samples; unfortunately the availability of only two points put limitations on the accuracy of the estimations of transition periods for different temperatures. Yet, the data collected painted a better picture of the transition zones. However, there is a need to perform many more experiments if an accurate model is to be developed to predict transition at various times and temperatures. But a conclusion can be made that as the temperature is decreased, the window of time during which the ductile to brittle transition occurs becomes larger.

Chapter 4. Single Edged Notched Bending

4.1 Introduction

Tests were performed on 25% and 50% plastically compressed samples aged at 105°C and tested in quasi static three point bending using Single Edged Notch Bending (SENB) samples. These were done to complement SENB 25% and 50% plastically compressed polycarbonate samples aged at 125°C by Strabala [1]. As the results from the Charpy experiments, it was determined that at 105°C we could thermally age the sample to induce a transition in the t samples from the toughened state brought about by plastic compression. The transition simply occurred faster at the higher temperatures [3, 23]. This profound effect of temperature was seen in the results from the Charpy tests and it would be expected that the same effect would be seen in the SENB tests. Samples were prepared and tested according to the methods used by Strabala [1].

4.2 Procedure

The SENB samples were prepared from sheets of GE Lexan polycarbonate. Samples were compressed to 25% and 50% plastic compression to be compared with uncompressed polycarbonate samples. After compression, samples were aged at 105°C and 125°C before final machining to avoid warping. The aging times for 105°C were 300, 700, 1500, 3000 and 6000 hours. The aging times for 125°C were 20, 50, 100 and 300 hours [1].

After aging, samples were machined to final dimensions of 10 mm x 80 mm x 4 mm, that were the same dimensions used for the Charpy samples. Furthermore, like the Charpy samples, SENB samples were machined in two orientations TA and TT. After the samples were machined, displacement correction tests were performed by loading the samples with the support separation removed to determine deformation resulting from the loading fixture deformation and contact indentation. After correction tests a 4 mm notch was made in the samples before creating a 1 mm crack with a razor blade to create a total notched length of 5 mm. 45° edges were milled into to the samples as shown in Figure 7 to accommodate the CTOD tool.

SENB samples were tested on a three point bending setup, with the support arms 40 mm apart and the loading point centered between the two support arms. The tests were conducted with a constant displacement rate of 10 mm/min, with a preload of 5 N before the loading began.

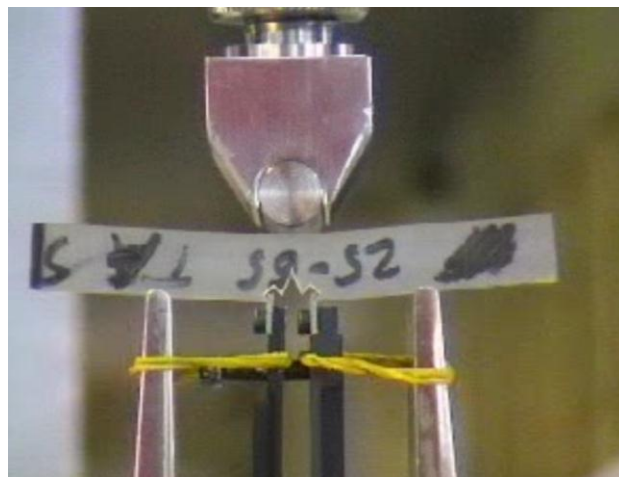


Figure 22: SENB Testing Apparatus

Load, load-line displacement and crack tip opening displacement (CTOD) were recorded by the Instron machine. Load-line displacement was corrected to compensate for the previously mentioned indentation deformation caused by the support arms. The correction was performed by measuring the amount of deformation as a function of its load and subtracting this from the load-line displacement at each data point. The load was also corrected by subtracting the initial preload from the total load to normalize the data.

With the corrected load-line displacement and load data, the energy dissipated by the sample was calculated using the trapezoid method to determine the total area under the curve. As was done by Strabala [1], data analysis was performed using load-line displacement up to 4.5 mm, for samples that broke in a ductile manner. All other samples with other failure modes broke before this point.

Additionally, a set of uncompressed SENB samples were annealed and quenched in the same manner as the CT samples before aging at 125°C.

4.3 Results

Figures 23 and 24 below show the energy dissipated by the compressed and aged polycarbonate samples before the samples failed. Figure 25 shows the load-displacement curves of examples of each failure type.

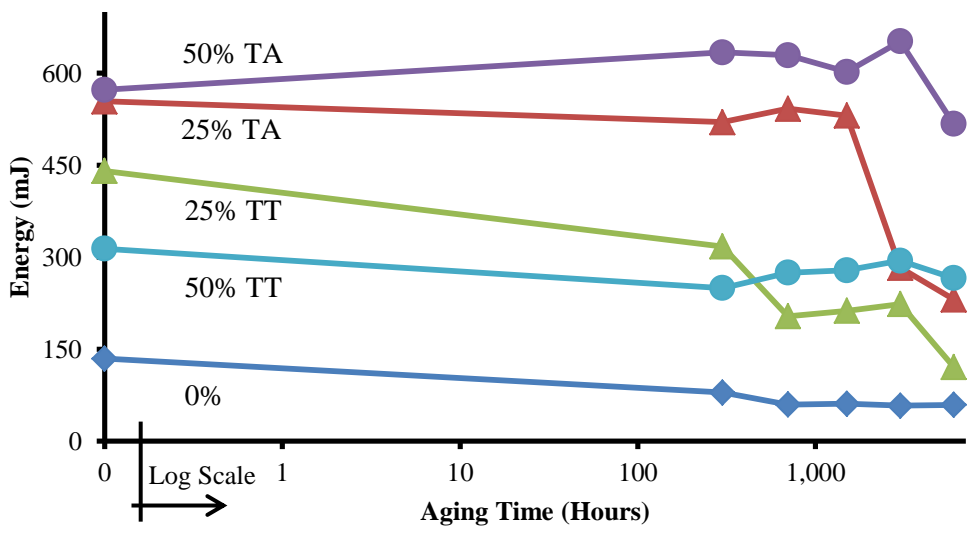


Figure 23: Energy dissipation of SENB samples Aged at 105°C. Combined data from Strabala [1] and Meagher.

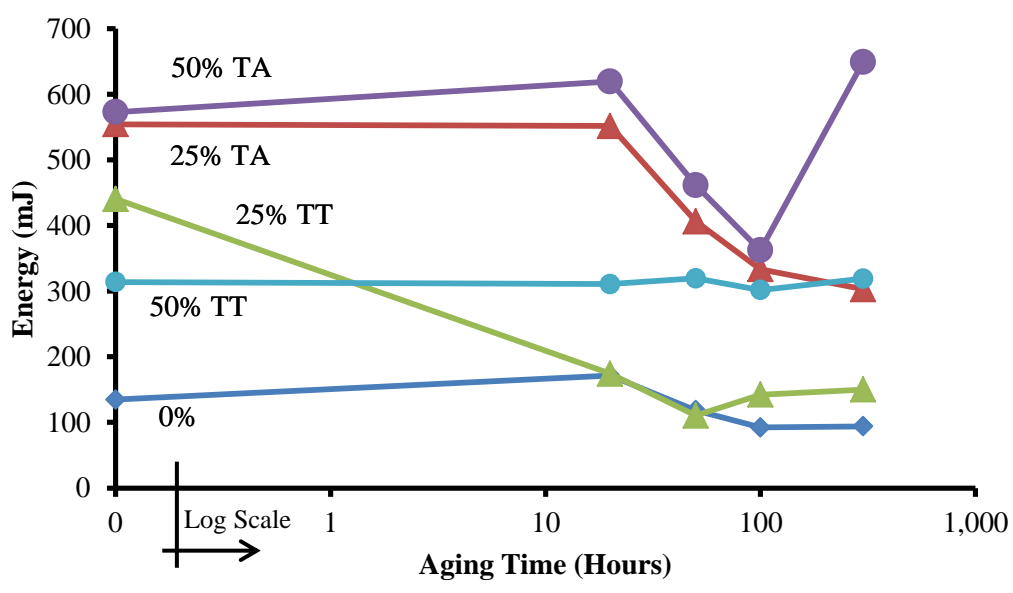


Figure 24: Energy dissipation of SENB samples aged at 125°C. Combined data from Strabala [1] and Meagher.

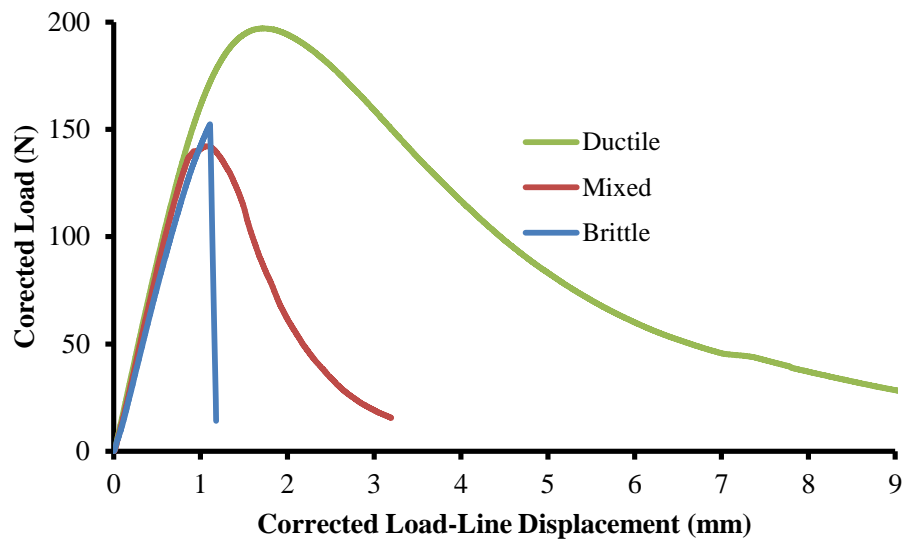


Figure 25: Load-displacement curves for each failure type.

In Figure 23 it can be seen that the 50% plastically compressed samples, both TA and TT, when aged at 105°C up to 6000 hours did not lose their induced toughness. To be specific, the average energy dissipation of these 50% compressed samples changes very little over the course of the aging and no samples underwent a brittle failure similar to the uncompressed samples. Likewise the behavior of the 50% TT samples that were aged at 125°C were equally consistent as those aged at 105°C; the average dissipated energy hovered around 300 mJ. There was however irregular behavior in the 50% TA samples aged at 125°C. While 0, 20 and 300 hour aged samples did not show a transition from the toughened state, there were samples aged at 50 and 100 hours that did break uncharacteristically, either in a brittle manner like the uncompressed samples or a mixed mode, like what is seen in the 50% TT samples.

The 25% compressed samples displayed the same behavioral pattern in the SENB tests as in the Charpy tests. Before aging, the 25% TA samples dissipated less energy

than the 50% samples of the same orientation, while the 25% TT samples dissipated more energy than the corresponding 50% TT samples.

The 25% TA samples aged at both 105°C and 125°C began to transition from their toughened state to a weak brittle state at longer aging times than the 25% TT samples. The 25% TT samples aged at 105°C began to transition after 700 hours of aging and the 25% TT samples aged at 125°C transitioned to an average energy dissipation similar to the uncompressed samples after 20 hours of aging, indicating an immediate loss of toughness in this orientation when aged at the higher temperature. The 25% TA underwent the same transition from their toughened states, but like the Charpy samples, the SENB samples began transitioning at a later times than their TT counterparts. For 25% TA samples aged at 105°C, the transition began at 3000 hours and the samples aged at 125°C began to transition after 50 hours of aging. The aging times where the transition begins to occur were consistent in both the Charpy and SENB tests for 25% plastically compressed samples at both aging temperatures for TA and TT orientations.

Figures 26 and 27 show the load line displacement at failure for the samples aged at 105°C and 125°C respectively.

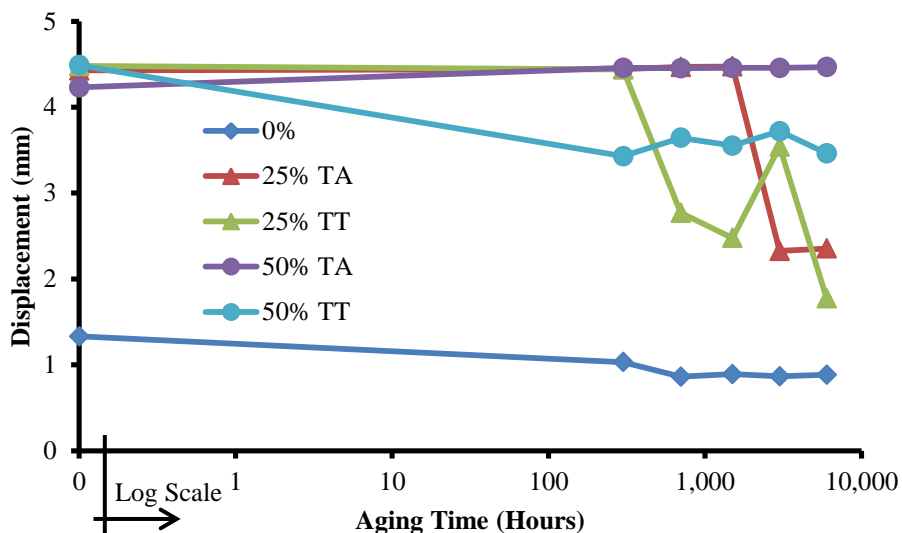


Figure 26: Corrected load-line displacement at failure of SENB samples aged at 105°C. Combined data from Strabala [1] and Meagher.

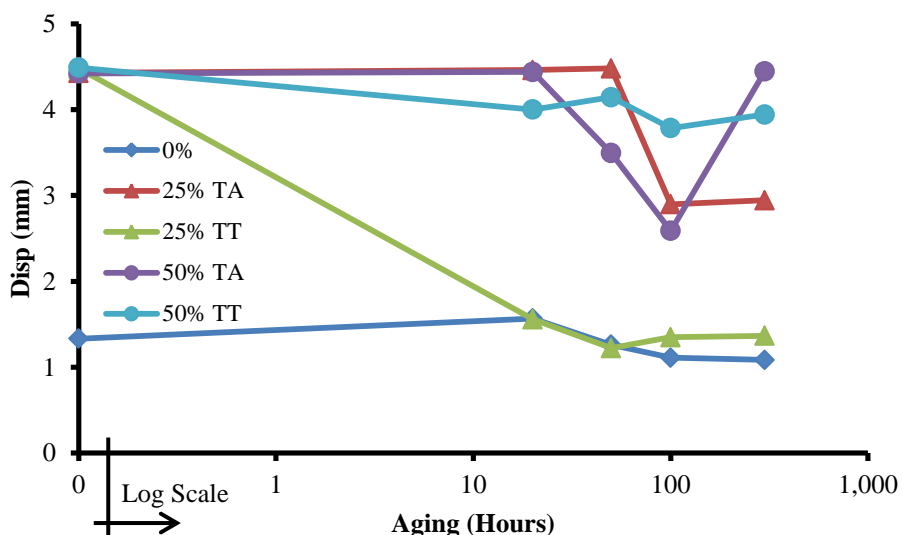


Figure 27: Corrected load-line displacement at failure of SENB samples aged at 125°C. Combined data from Strabala [1] and Meagher.

This value is indicative to the type of failure that the sample undergoes. Weak, brittle failures had a typical final load-line displacement of roughly 1-1.5 mm and did not exceed 2 mm. Failures that occurred at higher displacements but did not reach the testing limit of 4.5 mm and were characterized as a mixed failure that would not catastrophically break in a brittle manner but would tear with a crack propagation that was faster than a

pure ductile failure. The final ductile failure would result with a displacement well over 4.5 mm, but 4.5 mm was used as the upper threshold for processing and comparing data.

The load line displacement reinforces the failure behavior of the sample that was seen in the total energy dissipated. The 50% compressed TA samples that were aged at 105°C never failed at less than the cut-off of 4.5 mm, indicating ductile failure. Most of the 50% TA samples aged at 125°C had a ductile failure but it can be seen by the dip at 50 and 100 hours that some of these samples transitioned away from their toughened state. The 50% TT samples aged at 105°C never transitioned back down to a low load line displacement at failure but instead stayed relatively constant at around 3.5 mm at all aging times. Similarly, the 50% TT samples aged at 125°C never transitioned away from their toughened states. Though there was a slight drop-off that can be seen after 20 hours of aging at both temperatures, this was minimal. These results indicate the samples failed in a mixed mode similar to the behavior seen in the Charpy tests.

The 25% compressed samples behaved somewhat predictably when the Charpy results are considered. The 25% TA samples initially failed in a ductile manner, but began to transition after 3000 and 50 hours, respectively, of aging at 105°C and 125°C. This transition is seen in the average values that drop to about 2.5 mm of load line displacement at failure. The 25% TT also failed initially in a ductile manner with a maximum load-line displacement value of 4.5 mm, but transitioned from their toughened state after shorter times than the TA counterparts. The samples aged at 125°C transitioned fully to a brittle state after 20 hours, while the samples aged at 105°C began transitioning at 700 hours aging and were still in a transitioning phase at 6000 hours of aging.

Figures 28 and 29 display the Crack Tip Opening Displacement (CTOD) at failure for samples aged at 105°C and 125°C.

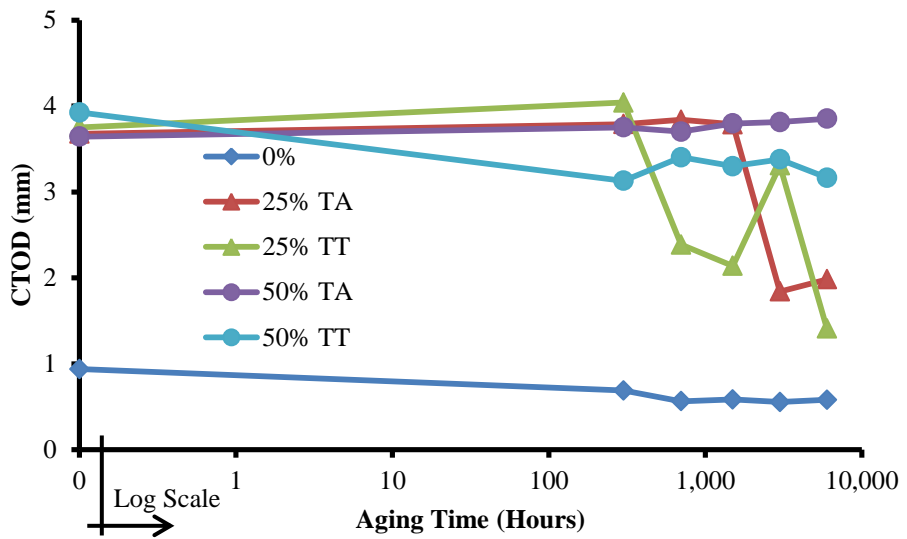


Figure 28: Crack tip opening displacement at failure of SENB samples Aged at 105°C. Combined data from Strabala [1] & Meagher.

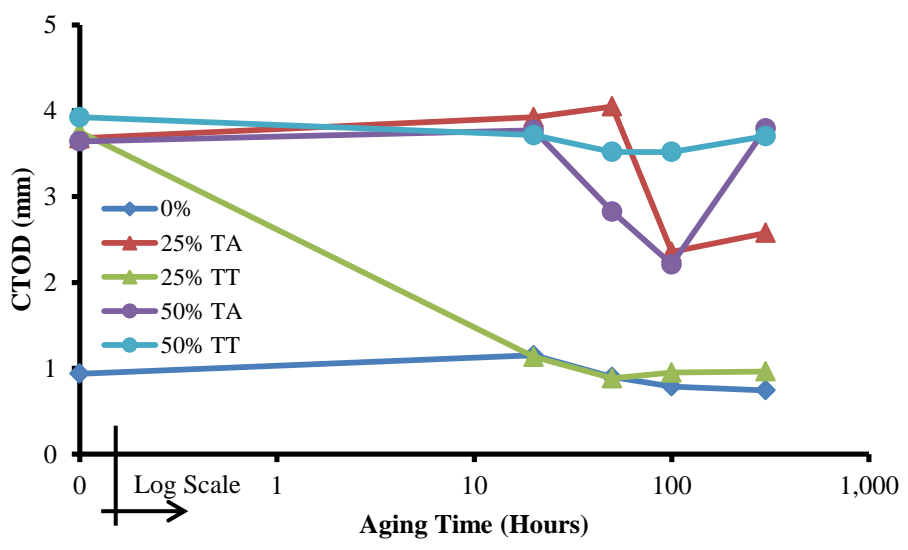


Figure 29: Crack tip opening displacement at failure of SENB samples aged at 125°C. Combined data from Strabala [1] & Meagher.

This value is indicative of how far the crack tip opening is displacing apart as the load line displacement increases. As can be seen from the Figures the behavior of the CTOD data is consistent with the behavior of the Load-Line Displacement data. Because of this, the CTOD value at the end of the test is indicative of the mode of failure of the samples.

The 50% samples aged at 105°C maintained consistent CTOD values after aging and never transitioned from their toughened states. The CTOD of the 50% TA samples were higher, about 3.75 mm, than the 50% TT samples, with an average CTOD of about 3.25 mm at failure. Furthermore it should be noted that the CTOD value of the 50% TA was stunted as the test was ended at a load line displacement of 4.5 mm. Additionally, the 50% samples aged at 125°C displayed a CTOD behavior consistent with its load line displacement values. The CTOD values of the 50% TA samples were roughly the same as those aged at 105°C except for some of the samples aged at 50 and 100 hours whose lowered CTOD values are indicative of the samples which transitioned away from their toughened state and broke in either a mixed or brittle mode. The CTOD values of the 50% TT samples were high before aging and did not transition away from the toughened state, in the same manner as the load line displacement measurements. And along with the load line displacement measurements, the CTOD measurements of the 50% TT are indicative of the mixed failure mode.

The 25% CTOD measurements behaved just as the load line displacement did. The CTOD measurements show a transitions beginning at 700 and 3000 hours at 105°C aging for 25% TT and 25% TA samples respectively. Furthermore, CTOD

measurements of the 25% TT and 25% TA samples aged at 125°C show the transitions from their toughened states beginning after 20 and 50 hours respectively.

4.4 Discussion

While the SENB samples generally behaved like the corresponding Charpy samples, there were certain unexpected occurrences that included the behavior of 50% TA compressed samples aged at 125°C. A few TA samples aged for 50 and 100 hours underwent a transition from their toughened state that was not seen in the 50% samples aged at 105°C.

On the other hand, the 50% compressed samples aged at 105°C and the 50% TT samples aged at 125°C behaved much like the Charpy samples in that they did not transition from their toughened state. This consistency with the Charpy tests among a vast majority of the 50% compressed samples would lead to a conclusion that the higher compression samples maintain their toughness equally well under quasi static and dynamic loading situations. However, to solidify this conclusion it is necessary to quantify the statistical significance of the few 50% TA samples which did transition from their toughened state and broke with lower energy dissipation.

In addition, the 25% compressed samples aged at 125°C behaved much in the same way that their Charpy counterparts did. They began to transition from their toughened states in the same manner. As did the 25% compressed samples aged at 105°C.

So while the behavior of the SENB tests would seem to reinforce the conclusions made from the Charpy tests, where the 50% compressed samples are more resistant to

transitioning from their toughened state than the 25% compressed samples. The transitioning of a few 50% TA samples aged at 125°C raises the point that more tests need to be done to produce statistically significant data that can provide a solid conclusion to the resistance to aging of 50% compressed samples compared to lower compressed samples.

The behavior of the 50% compressed samples added some complication to the conclusions regarding their ability to resist transitioning from toughened states to a brittle state due to physical aging. Other conclusions regarding the anisotropy of energy dissipation dependent on the orientation and compression level were confirmed.

As was the case in the Charpy tests, the amount of energy dissipated in unaged samples was greatest in the 50% TA samples followed by 25% TA samples. Furthermore, the anisotropy was also greater in the 50% samples where the difference of energy dissipation between the TA and TT orientations was greater than the energy dissipation difference of the unaged 25% samples. The difference between the 50% samples was so much greater that the 25% TT samples were actually tougher than the 50% TT.

With respect to the transition period of the SENB samples, it was seen that the TA samples began to transition from their toughened states after longer aging times than their TT counterparts. This occurred in the samples aged at both 105°C and 125°C.

Additionally, before any transition occurred, the failure modes of SENB samples were the same as the Charpy samples of the same compressions and orientations. The uncompressed samples failed in a brittle manner indicative of tensile failure. The TA samples failed in a ductile manner indicating tearing from shear stresses. While the TT

samples displayed a mixture of the two failure modes indicating a mixture of shear and tensile failure

Chapter 5. Compact Tension Tests

5.1 Introduction

In addition to the SENB tests, a second set of quasi-static loading tests were performed on samples that were annealed and quenched before compression and which were using a smaller sample that could be cut along all possible orientations. It has been shown that annealing polycarbonate above its glass transition temperature and then quickly cooling by quenching in water creates internal stresses shown to toughen the samples [14]. The SENB samples were not annealed and quenched before compression; the following CT tests were performed on annealed and quenched samples to compare their behavior with that of the SENB samples.

Unfortunately, there were no bars readily available that could be used to make more SENB samples. Instead there were many cylinders that had been annealed and quenched before plastic compression and were available to use. And while they were not large enough to make SENB samples they were large enough to make CT samples. Standards ASTM E1820 [30] was used to specify CT sample size. However, the mounting holes were drilled smaller to fit the mounting hardware and the notch opening was simplified to allow for easier machining. Indentation correction was performed according to ASTM D5045 [31]. Tension testing used the same method as Strabala [1], but with the differences being a higher preload, 7 N, and the samples were broken in tension.

5.2 Procedure

Before compression, the PC cylinders were annealed and quenched according to the following procedure:

1. Held at 105°C for 3 days to remove water.
2. Annealed at 150°C for 2 hours.
3. Immediately quenched in room temperature water, ~23°C.

After annealing and quenching, rods were compressed to 15%, 25% and 35% plastic compression. Other samples were left uncompressed so as to have a baseline for the experiment. Samples were then cut and machined to a final dimension of 20mm x 20mm x 7 mm before the mounting holes and notches were made. After machining to final dimensions, the samples were then drilled with 2.5mm holes used to mount the samples on the Instron's holders. After holes were drilled, data correction tests were performed by loading the un-notched samples to measure the amount of displacement at the loading points. This correction test is displayed in Figure 30. This displacement was used to interpolate the amount of displacement that needed to be subtracted at each point of the final test dependent upon the load value. After indentation displacement correction measurements were performed on the samples, the crack was made by first machining a slot 12mm in length followed by notching a 2 mm crack with a razor blade. The detailed diagram of this sample can be seen in Figure 9 in Chapter 2.

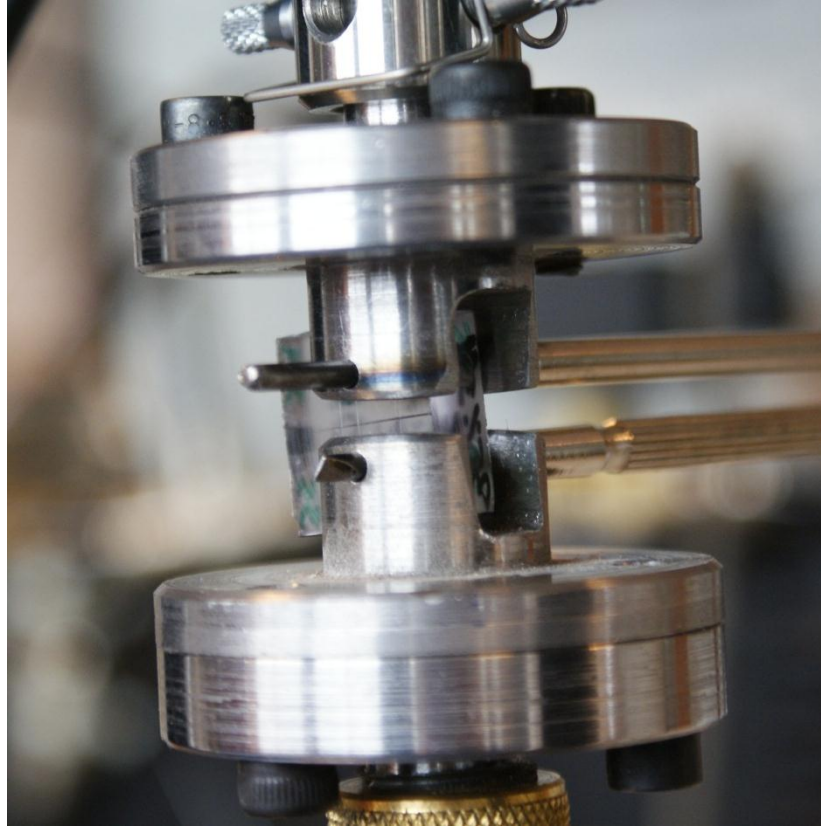


Figure 30: Data correction test on un-notched CT sample.

There were three orientations tested using the CT samples. The first orientation, TT, was transversely cut and transversely notched with respect to the axis of compression. The second orientation was the AT orientation that was axially cut and transversely notched with respect to the axis of compression. The third orientation was the TA orientation and was transversely cut and axially notched with respect to the axis of compression. A detailed diagram of each of the three orientations is shown in Figure 11 in chapter 2.

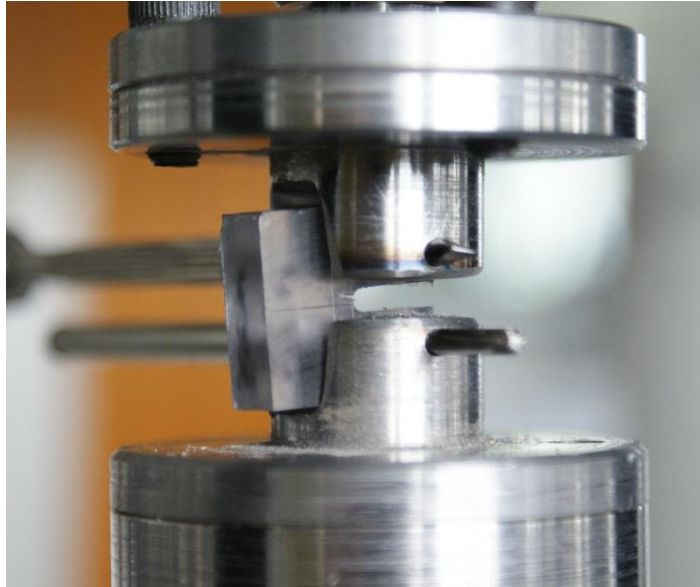


Figure 31: CT testing apparatus

After correction tests and notching was performed, samples were deformed and broken in tension at a constant rate of displacement of 10 mm/min after undergoing a preload of 7 N. This process is shown in Figures 31 and 32. Load and load-line displacement were recorded. Corrected load-line displacement was calculated using an interpolated correction factor obtained from the displacement correction tests. The total energy dissipated was calculated using the trapezoid method to find the area under the load/corrected displacement plot. As the SENB tests used a maximum allowable load-line displacement of 4.5 mm for calculating energy dissipated, so too did the CT samples use a maximum displacement. However, in the case of the CT samples the maximum displacement was 9 mm.

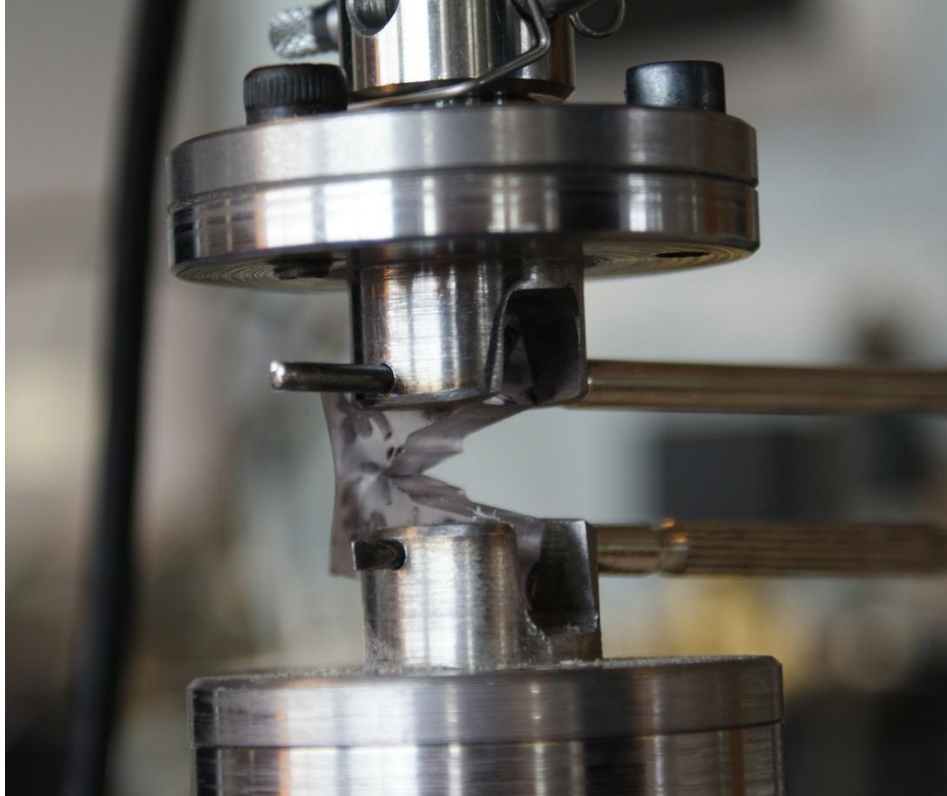


Figure 32: Ductile failure of CT sample.

5.3 Results

Figures 33, 34 and 35 show the dissipated energy at failure of the CT samples.

Figure 36 shows the load-displacement graph of the three various failure types.

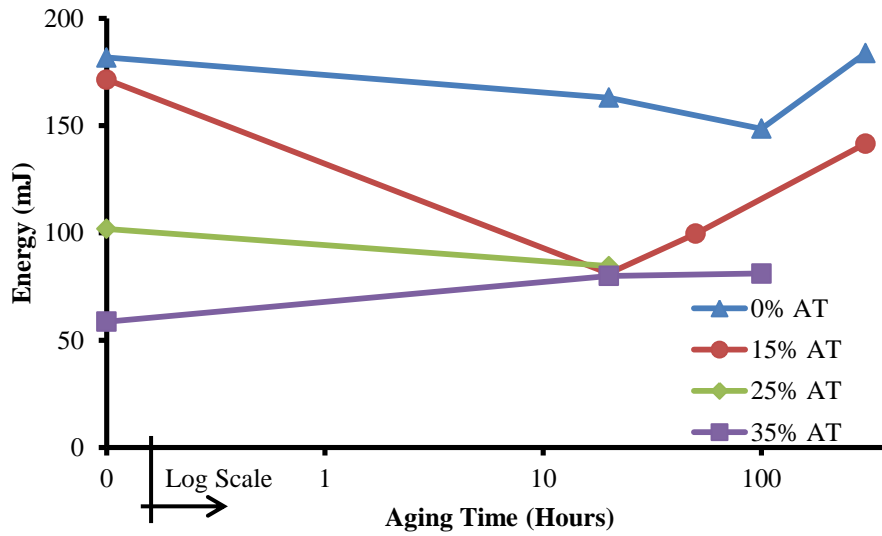


Figure 33: Dissipated energy of AT oriented CT samples.

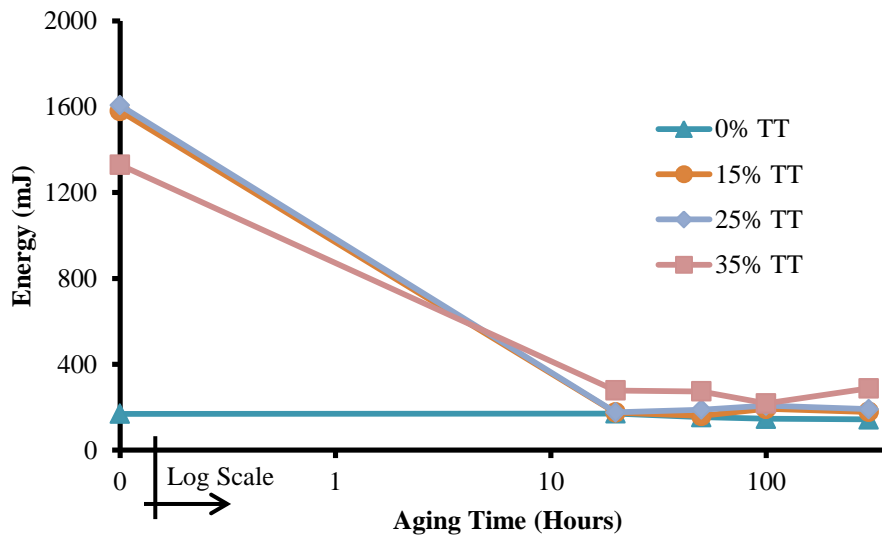


Figure 34: Dissipated energy of TT oriented CT samples.

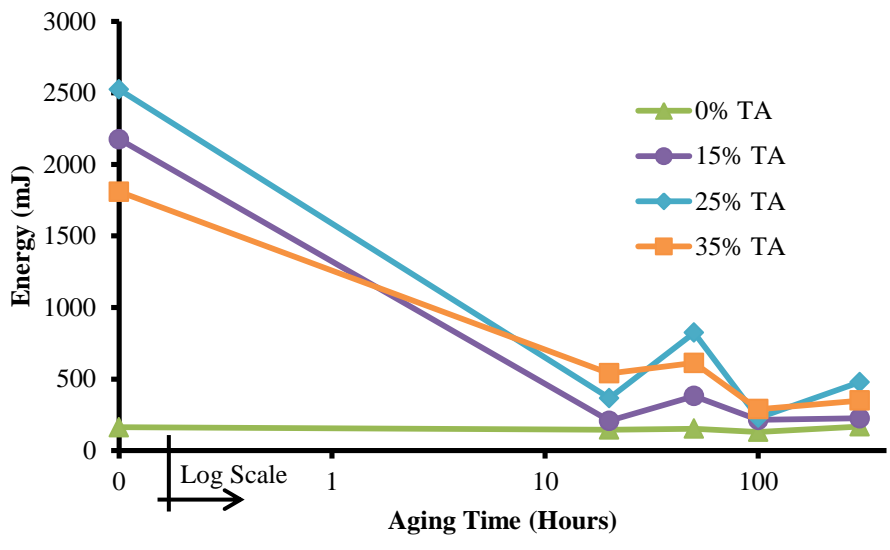


Figure 35: Dissipated energy of TA oriented CT samples.

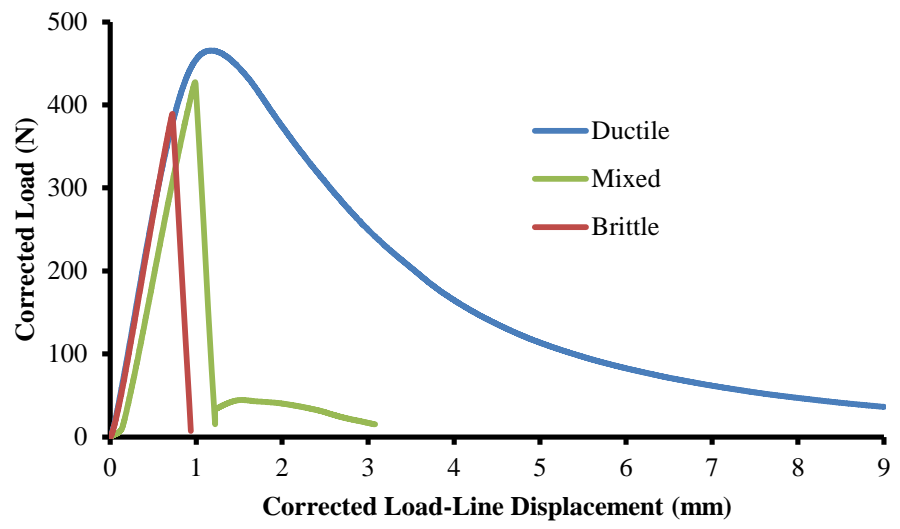


Figure 36: Displacement-load graph of three failure modes.

Like the Charpy and SENB tests discussed previously, the uncompressed samples of broke in a brittle mode and then proceeded to continue to break in a brittle manner at all aging times. The orientation of the uncompressed samples all displayed the same behavior before and after aging regardless of orientation. While it can be seen that the

compressed samples (15%, 25%, and 35%) dissipated more energy in both the TA and TT orientations, these compressed samples dissipated less energy in the AT orientation than the uncompressed samples at all aging times.

It is evident that Figure 33, displaying the energy dissipation data of AT oriented samples, is missing several data points compared to Figures 33 & 34. This is because many of the AT oriented samples fractured while the razor notch was added. Specifically 2 uncompressed samples, 4 samples with 15% compression, 7 samples with 25% compression, and 6 samples of 35% compression were lost during notching. Only 2 total samples of the other orientations fractured during notching, 1 TA sample and 1 TT sample. This indicates that not only is the AT orientation generally weaker than the other two orientations tested, but that compression negatively affects the toughness of the polycarbonate in this specific orientation.

This weakening effect caused by compression on failure of AT oriented samples was then confirmed by the total energy dissipation of the samples. As the level of plastic compression increased, the dissipated energy of the AT oriented samples decreased. All of the samples in this orientation failed in a brittle manner, but the higher compressed samples were more prone to breaking at lower loads and displacements, which resulted in lower energy dissipation.

The energy dissipation results of TT oriented samples were somewhat more predictable. Unlike the AT samples, the compressed TT oriented samples became tougher. All compressed TT samples failed in a ductile manner. These samples did not follow the trend of becoming tougher with increased compression that was observed in the SENB and Charpy tests. Instead the 35% compressed samples had lower average

energy dissipation than both the 15% and 25% compressed samples. The 35% compressed samples had an initial energy dissipation of 1330 mJ while the 15% and 25% compressed samples respectively had energy dissipations of 1580 mJ and 1606 mJ.

After the TT compressed samples were aged for 20 hours at 125°C, all began to transition away from their toughened states. The 15% and 25% compressed samples generally failed with average energy dissipation near 200 mJ, while the 35% compressed samples generally failed with an average energy dissipation of around 270 mJ, though with higher standard deviations.

The TA oriented samples behaved similarly to the TT oriented samples. The uncompressed samples failed in a brittle manner with an average energy dissipation of generally close to 150 mJ at the various aging times. The compressed samples failed in a toughened ductile state before aging, but failed with higher energy dissipations than their TT oriented counterparts. The 15% compressed samples failed with an average energy dissipation of 2180 mJ, the 25% compressed samples failed at 2520 mJ and the 35% samples failed at 1810 mJ. Furthermore, after aging times of 20 hours, the TA oriented samples began to transition away from their toughened states.

5.4 Discussion

It was possible to compare the SENB tests with the Charpy tests, as they were performed on samples that were prepared from the same sheets of polycarbonate and same preparation, aside from their respective notching of course. The tests performed on the CT samples were in addition preconditioned by annealing and quenching. As a result,

the CT tests cannot be directly compared to the SENB and Charpy tests. Yet, the CT tests provided samples from all three sample orientations possible.

As discussed in the results, the compressed samples became tougher as a result of the plastic compression in the TA and TT orientations while the AT oriented samples became weaker with compression. Specifically the weakest samples in the case of the AT oriented samples were the 35% compressed samples, the highest compression. 35% compressed samples were also weaker than their 15% and 25% compressed counterparts in the two other orientations TA and TT. The TA samples were toughest of the three orientations. While it would be expected that the higher compressed samples would be weaker in the TT orientation, as they were in the Charpy and SENB tests, it would seem uncharacteristic for the higher compressed samples to be weaker when the crack is oriented axial to the direction of compression. This is perhaps indicative that samples which have been annealed and quenched respond well to limited compression, but higher compressions such as 35% or greater do not provide further benefit.

As a result of aging, all of the compressed samples in the TA and TT orientations began to transition away from their toughened states after a shortest aging time, 20 hours at 125°C. Again this behavior is uncharacteristic as there is no anisotropy in the aging times required for transition in various orientations.

While the quantitative results of the CT tests cannot be compared with the results of the SENB and Charpy tests due to the difference in sample geometry and preconditioning, they seem to indicate that there is a fundamental behavioral difference in the way that the annealed and quenched samples react to plastic compression

Chapter 6. Summary and Conclusion

In this work it was demonstrated that PC samples toughened by compression display anisotropic behavior depending on the orientation that the crack will run in a fracture sample. In particular, cracks moving along the compressive axis consistently displayed greater energy dissipation than those moving perpendicular to the compression direction. As was shown in the CT samples, there is even a more dramatic difference between the TT and AT samples, with the axially cut AT samples displaying no increase in toughness as a result of plastic compression. Additionally, in the Charpy and SENB samples the anisotropic difference in toughness between the two orientations TA and TT increased dramatically as plastic compression increased from 25% to 50%.

Each orientation AT, TT and TA had its own characteristic failure mode. As was mentioned earlier, the AT was brittle which indicated tensile forces causing the failure. The TT was a mixed mode, which had a fracture surface indicating both brittle failure from tensile failure and plastic flow from shearing. And the TA samples broke in a ductile manner indicating shear failure.

The PC polymer chains undergo deformation when the sample is compressed and result in the reorientation of the chains toward the perpendicular to the axis of compression. This orientating of polymer chains when loaded creates a different structure that the cracks must pass through or around depending upon the sample orientation. The orientation of the chains with respect to the crack propagation

determines the method of failure. It is recommended that future research study the morphology change along the various orientations in PC samples which have been highly compressed.

In samples that were not annealed and quenched before compression (Charpy and SENB), the anisotropic behavior of the compressed polycarbonate was not simply limited to the difference in toughness dependent on orientation. There was also a distinct anisotropy with respect to the amount of aging time required to induce a ductile to brittle failure transition dependent upon crack orientation. In both the Charpy and SENB samples the 25% compressed samples in the TT orientation underwent a transition well before the TA samples of the same compression and aged either at 105 °C or 125 °C. The 50% samples showed a very interesting behavior in that they were very resistant to transitioning from ductile to brittle after aging. This indicates that the molecular reorganization of polymer chains becomes slowed as the plastic compression increases.

As was seen in the Charpy samples the toughness that was gained as a result of the plastic flow was lost in the 25% compressed samples after aging at temperatures below the glass-transition temperatures. After this loss had occurred due to aging, the samples broke with roughly the same energy dissipation and brittle failure mode as the uncompressed samples. Samples broken with cracks running along the transverse direction experienced this loss much sooner than the other samples (after 1-2 hours at 125 °C), while the samples broken with cracks running along the axial direction took longer to lose their increased toughness (after 50 hours at 125 °C). This transition occurs at longer aging times as the aging temperature was decreased and at shorter aging times when the aging temperature was increased, indicating a temperature dependence of these

transitions. In the case of the 50% compressed samples, the majority of the increase in energy loss was maintained at all aging times tested with what seems to be a significant suppression of any fracture mode transition.

In samples that did transition from their toughened states, the transition was bimodal. The samples would either fail at their toughened state or would revert fully to the undeformed state. Furthermore, after performing ultrasonic wave speed measurements on the samples, there was a significant drop in the longitudinal wave speed for certain samples, specifically those with 25% compression.

Future Work

There is still a limited amount of data from the tests performed, specifically with regards to the statistical behavior of samples transitioning from toughened to brittle fracture and the effect of aging temperature on rate of transition from toughened state. As such it is important that further studies perform more fracture experiments. With that being said it would be wise for future projects to focus on a specific aging temperatures, compressions or orientations as there are a large number of experiments that must be performed to reach significant conclusions.

Furthermore, it is highly recommended that future tests study the change morphology and internal structure of PC after it has been deformed and subsequently aged. This is vital if we are to understand the mechanism that causes toughening and the mechanism that is responsible for causing the transition from toughened to brittle state.

Appendix A

SENB Load/Displacement Figures

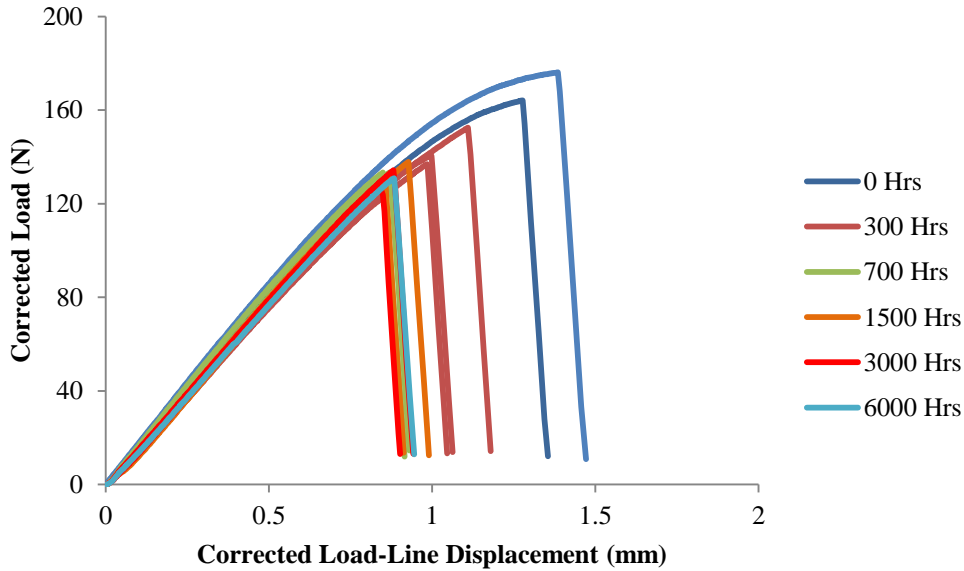


Figure 37: Corrected load/displacement curves of uncompressed SENB samples aged at 105°C. Combined data from Strabala [1] & Meagher.

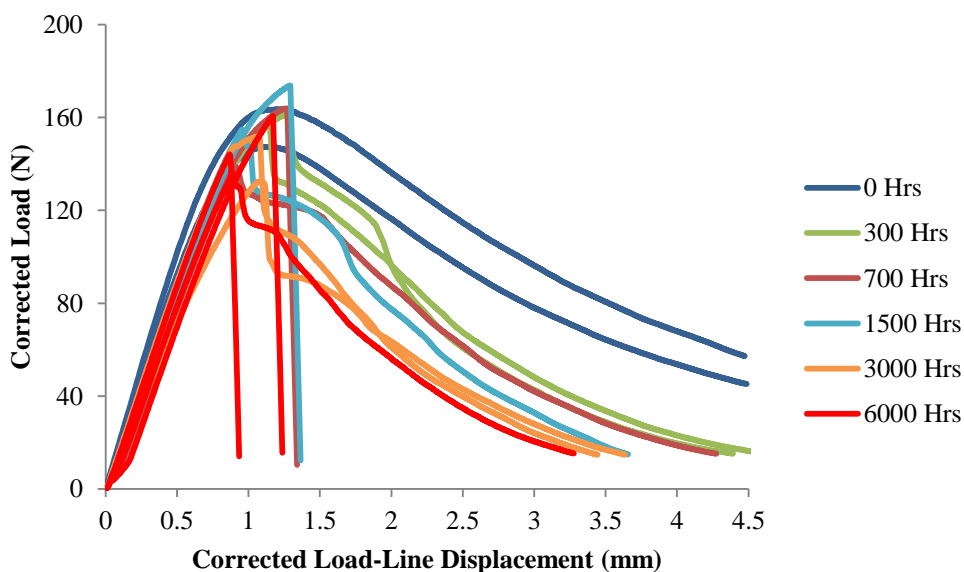


Figure 38: Corrected load/displacement curves of 25% compressed, TT oriented SENB samples aged at 105°C. Combined data from Strabala [1] & Meagher.

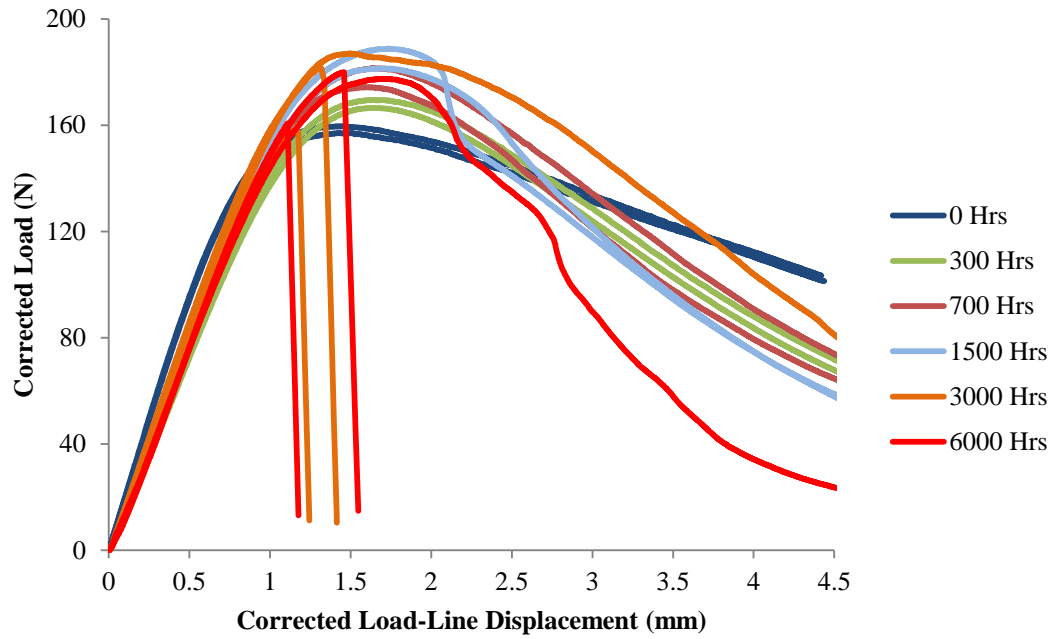


Figure 39: Corrected load/displacement curves of 25% compressed, TA oriented SENB samples aged at 105°C. Combined data from Strabala [1] & Meagher.

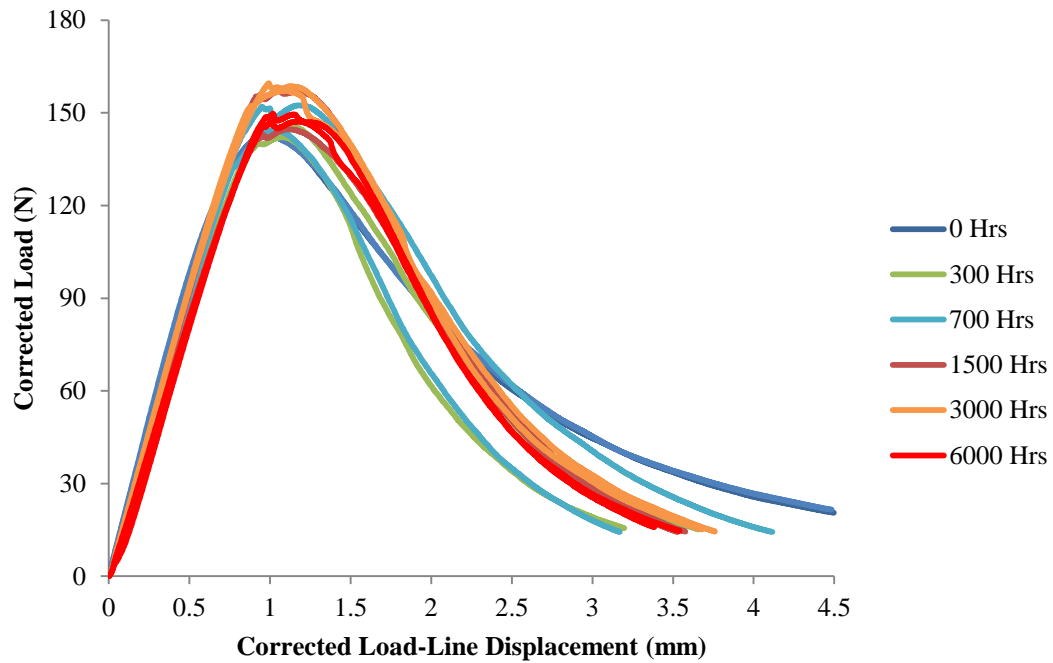


Figure 40: Corrected load/displacement curves of 50% compressed, TT oriented SENB samples aged at 105°C. Combined data from Strabala [1] & Meagher.

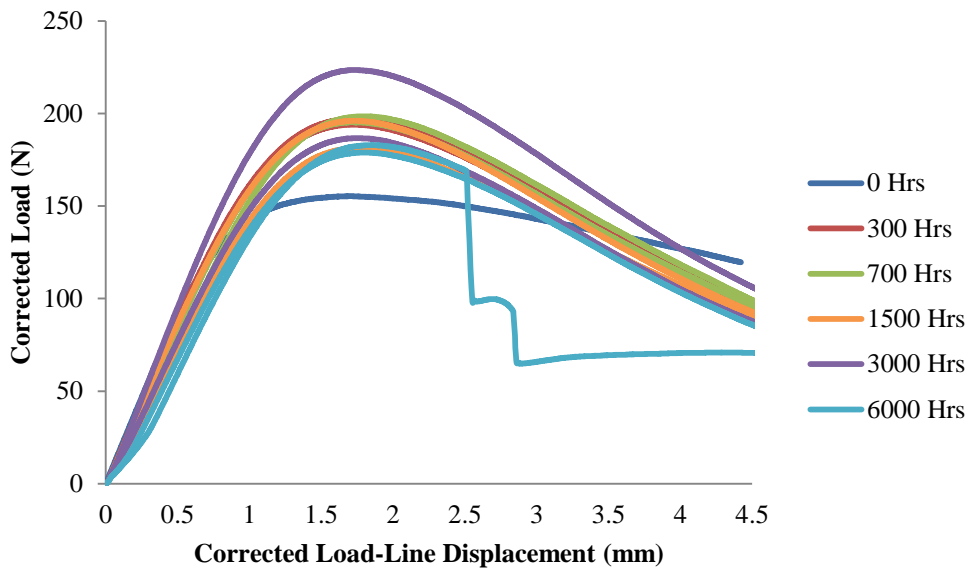


Figure 41: Corrected load/displacement curves of 50% compressed, TA oriented SENB samples aged at 105°C. Combined data from Strabala [1] & Meagher.

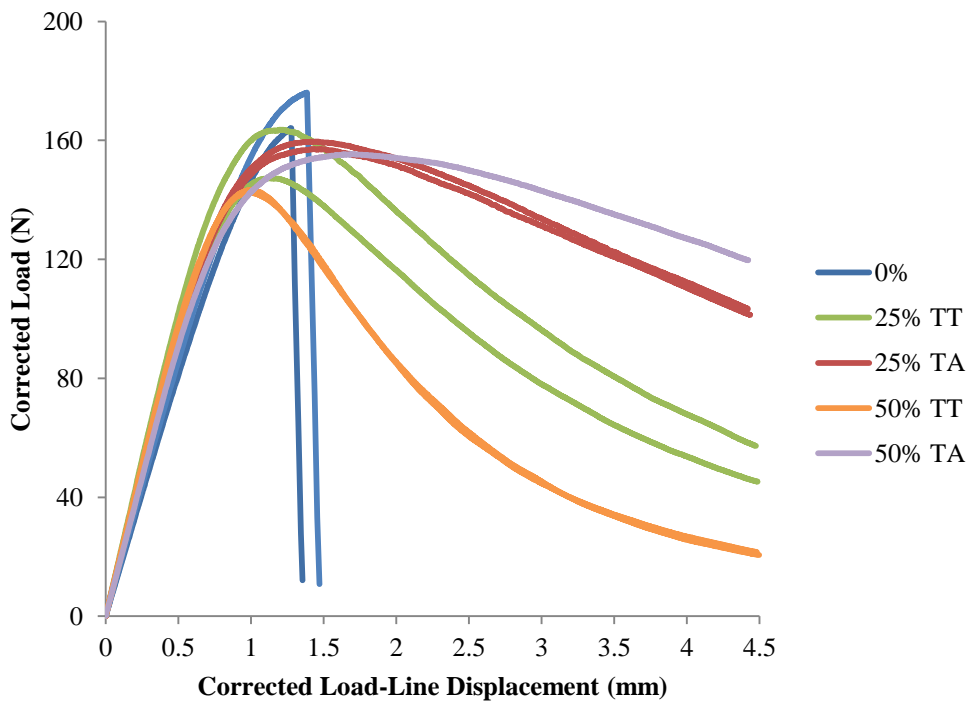


Figure 42: Corrected load/displacement curves of unaged SENB samples. Combined data from Strabala [1].

Appendix B

CT Load/Displacement Figures

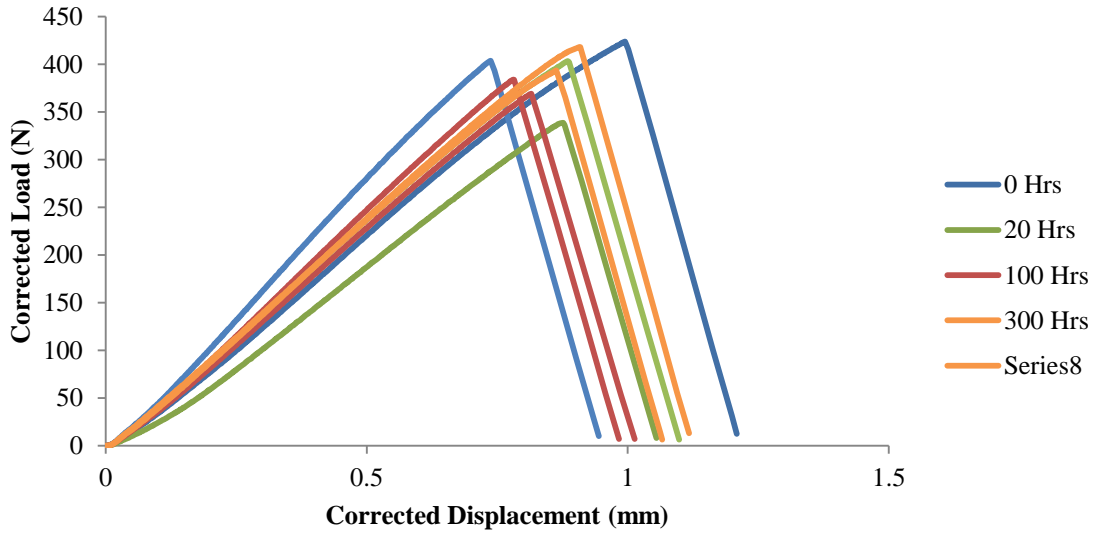


Figure 43: Corrected load/displacement curves of uncompressed, AT oriented CT samples, aged at 125°C.

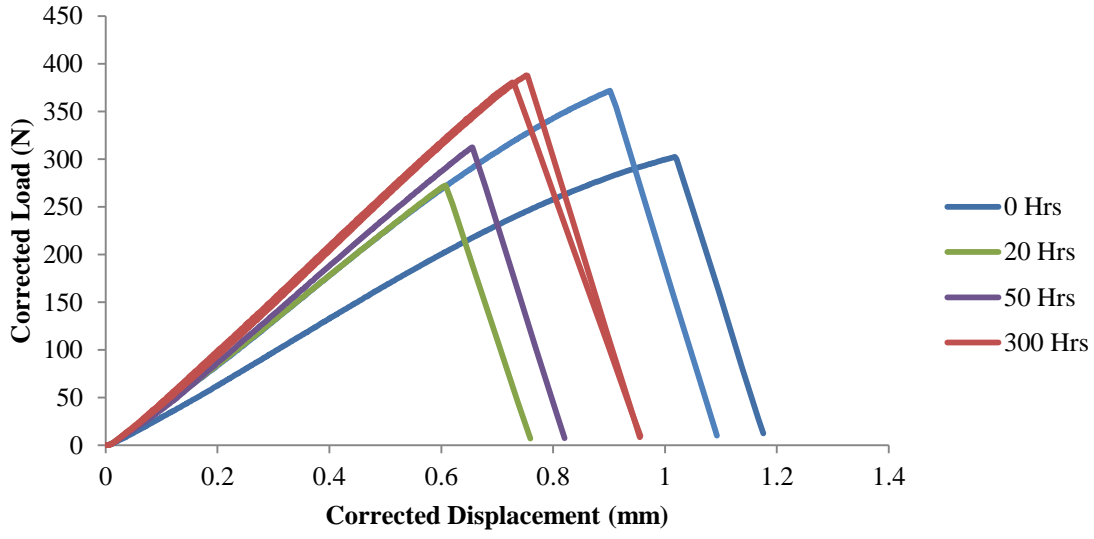


Figure 44: Corrected load/displacement curves of 15% compressed, AT oriented CT samples, aged at 125°C.

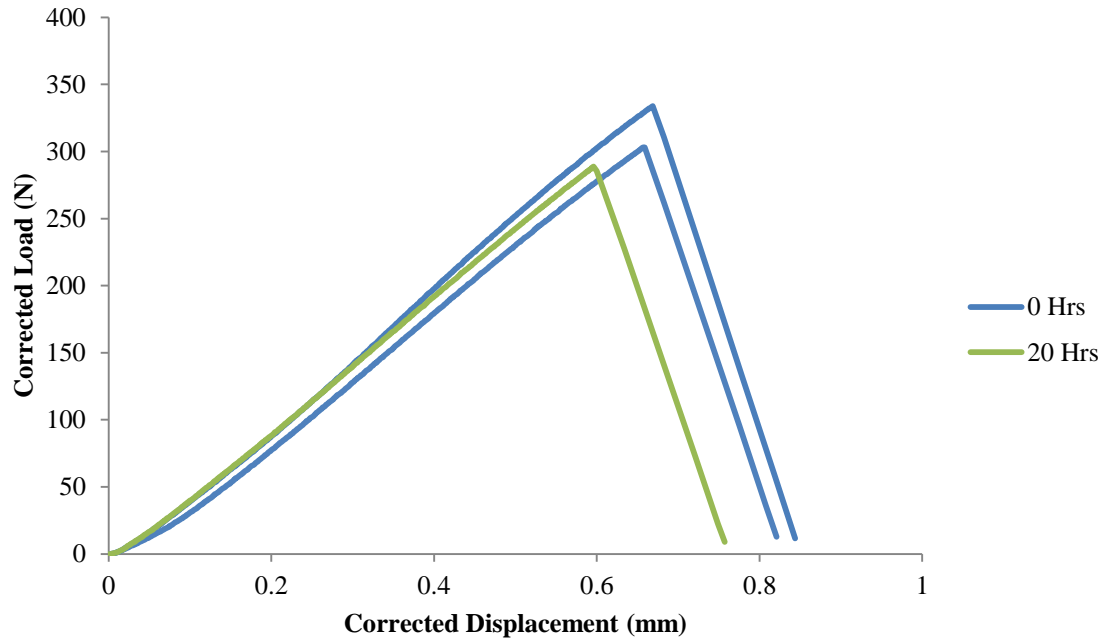


Figure 45: Corrected load/displacement curves of 25% compressed, AT oriented CT samples, aged at 125°C.

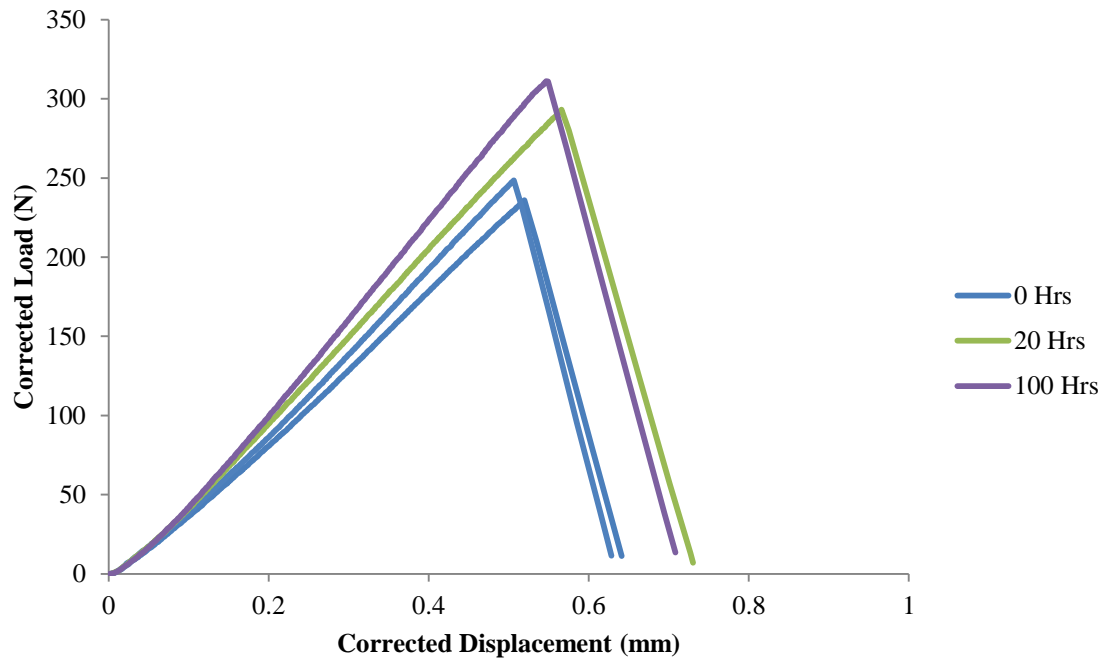


Figure 46: Corrected load/displacement curves of 35% compressed, AT oriented CT samples, aged at 125°C.

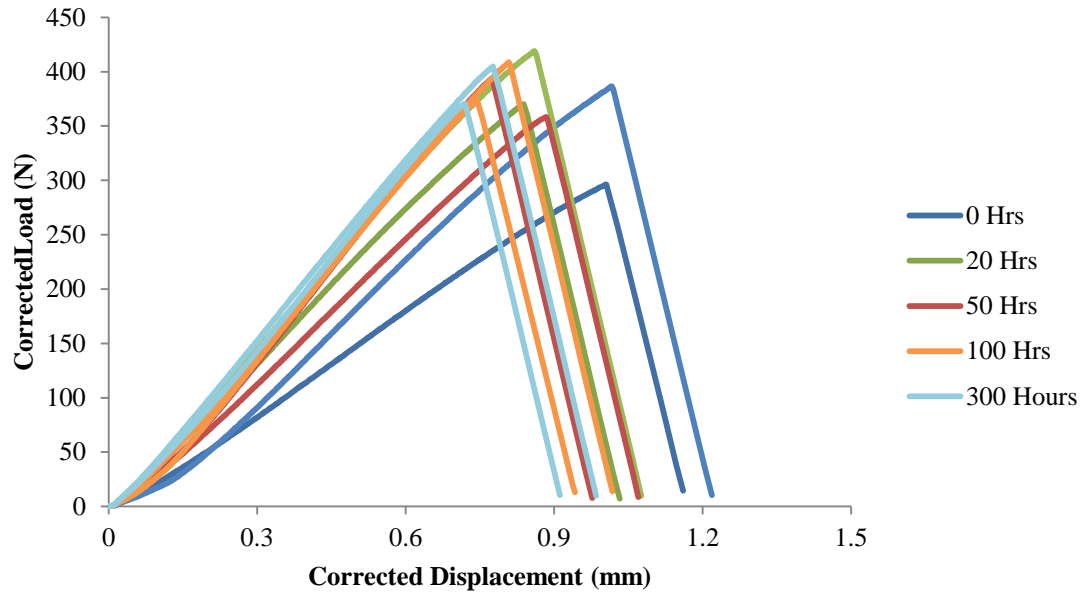


Figure 47: Corrected load/displacement curves of uncompressed, TT oriented CT samples, aged at 125°C.

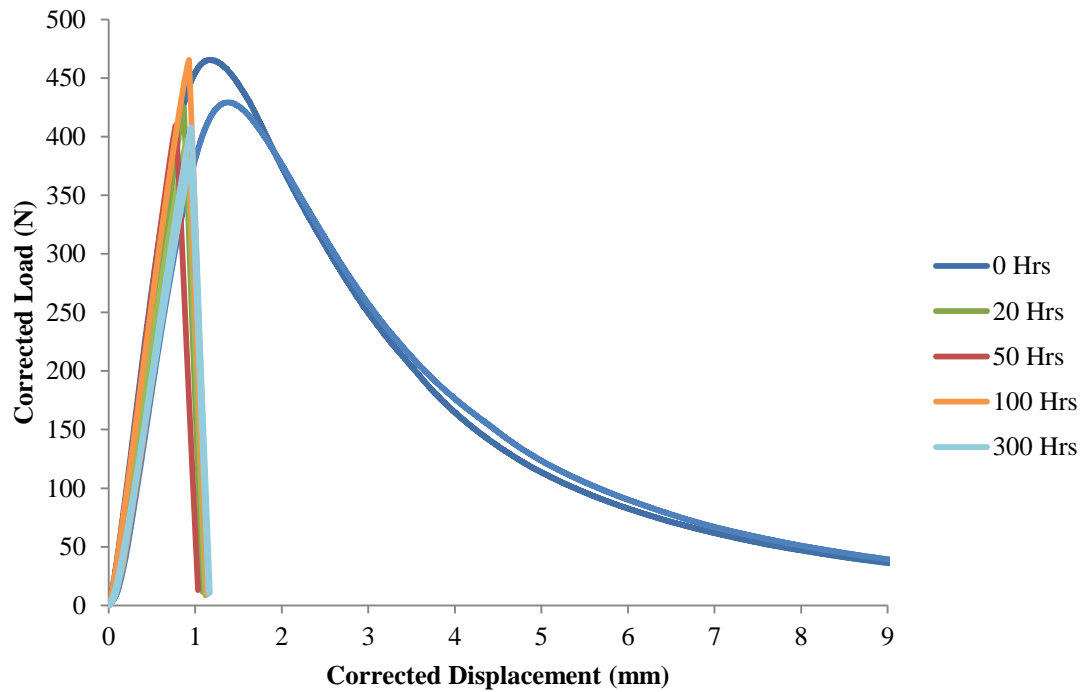


Figure 48: Corrected load/displacement curves of 15% compressed, TT oriented CT samples, aged at 125°C.

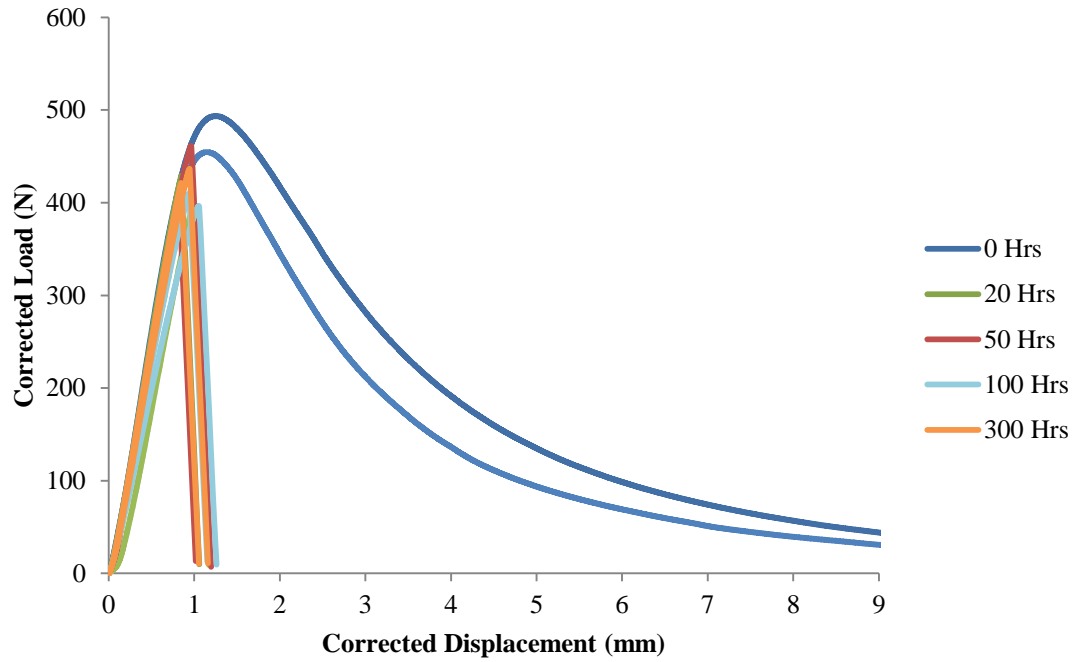


Figure 49: Corrected load/displacement curves of 25% compressed, TT oriented CT samples, aged at 125°C.

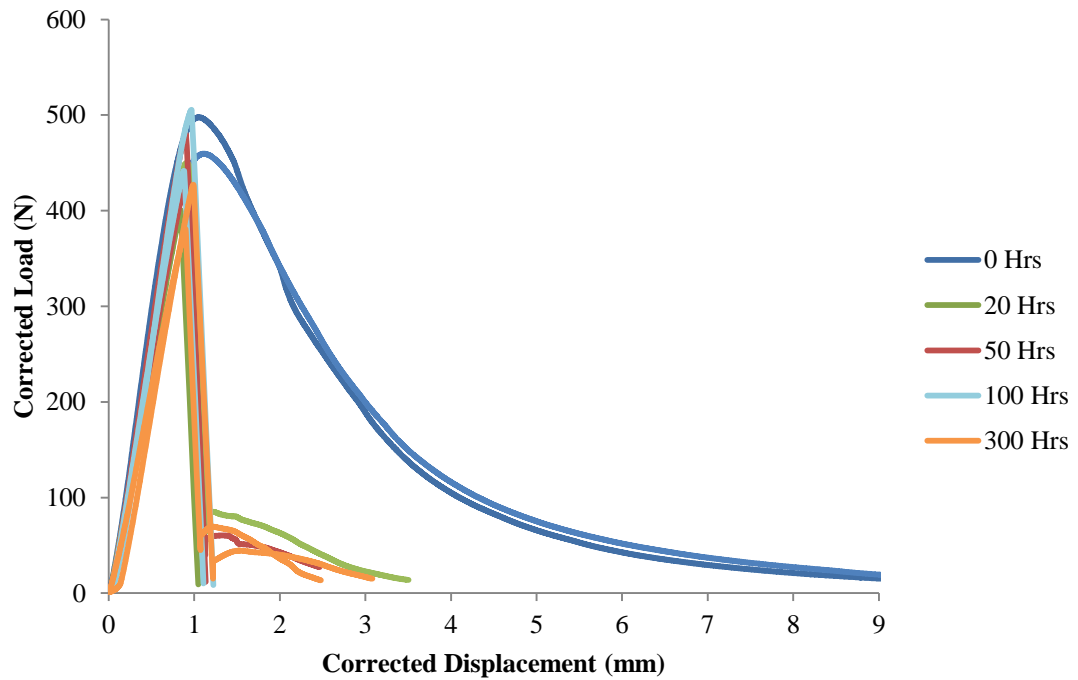


Figure 50: Corrected load/displacement curves of 35% compressed, TT oriented CT samples, aged at 125°C.

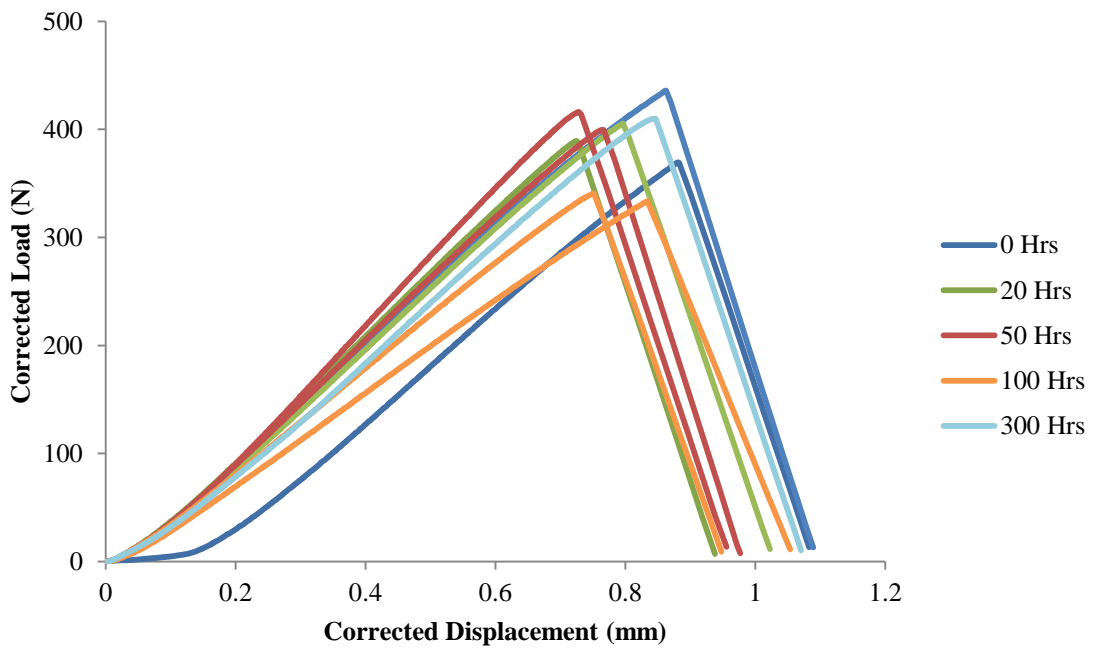


Figure 51: Corrected load/displacement curves of uncompressed, TA oriented CT samples, aged at 125°C.

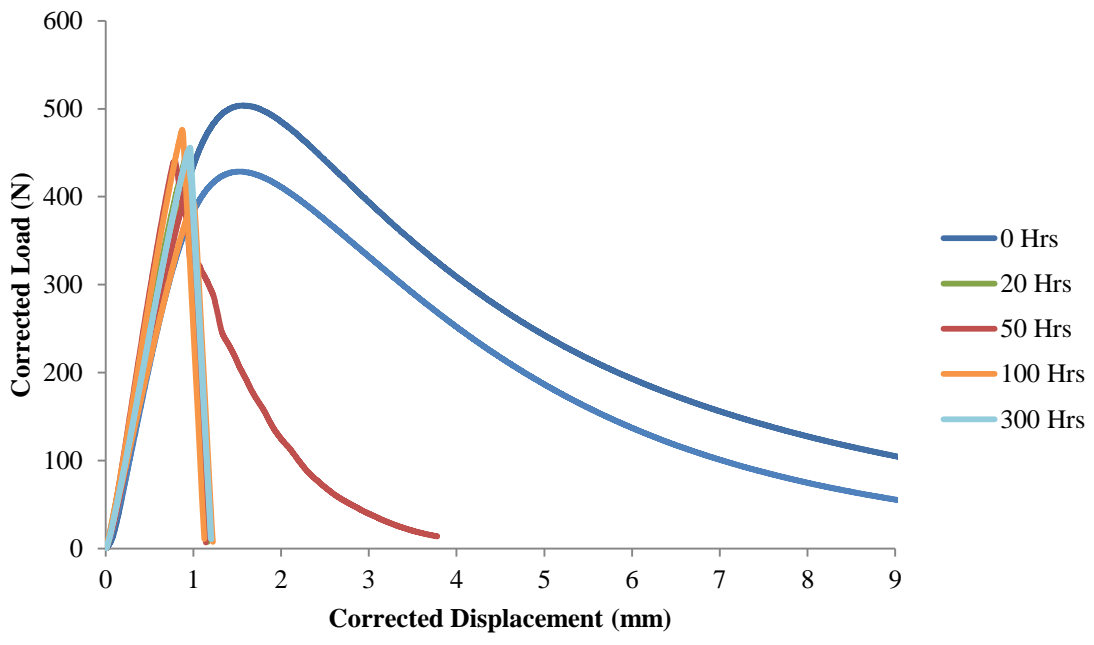


Figure 52: Corrected load/displacement curves of 15% compressed, TA oriented CT samples, aged at 125°C.

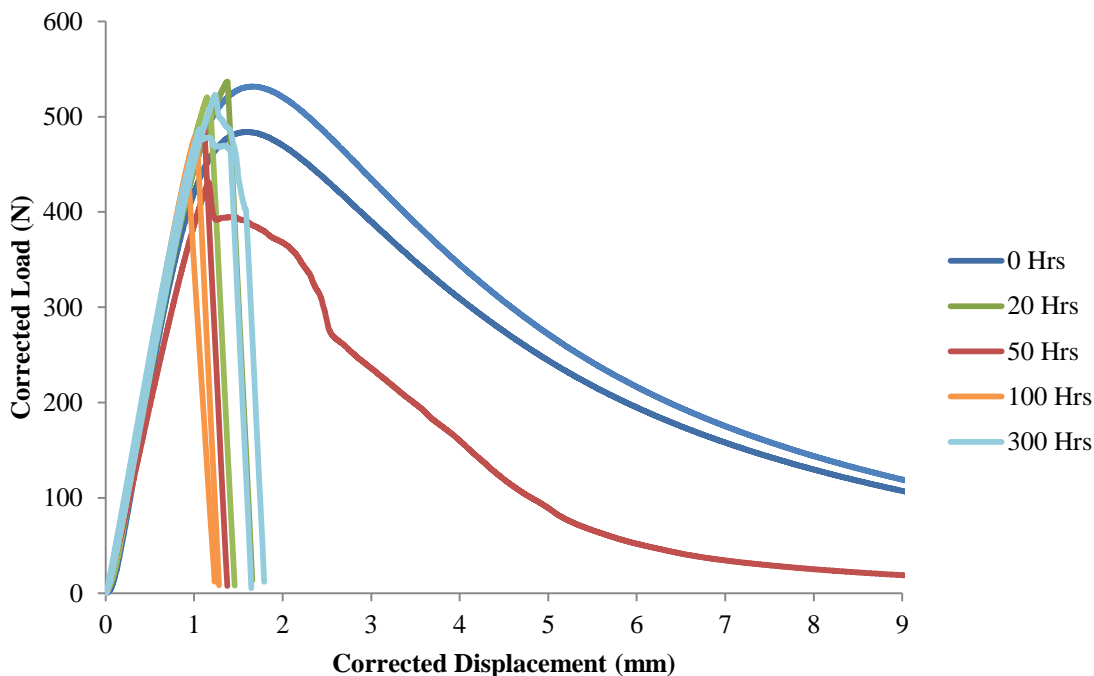


Figure 53: Corrected load/displacement curves of 25% compressed, TA oriented CT samples, aged at 125°C.

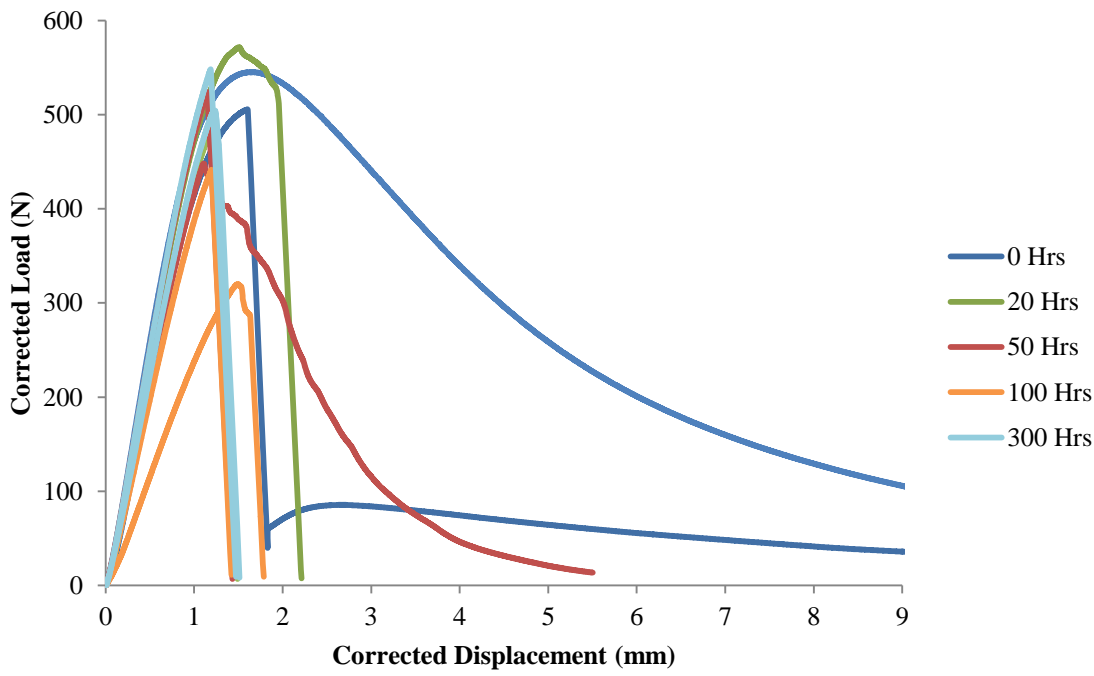


Figure 54: Corrected load/displacement curves of 35% compressed, TA oriented CT samples, aged at 125°C.

References

- [1] Strabala, K. W., “The Effects of Combined Compression and Aging on the Properties of Glassy Polycarbonate,” University of Nebraska-Lincoln, 2009.
- [2] “Polycarbonate,” 2010, Wikipedia Commons.
- [3] Thakkar, B. S., Broutman, L. J., and Kalpakjian, S., “Impact strength of polymers 2: The effect of cold working and residual stress in polycarbonates,” *Polymer Engineering and Science*, Vol. 20, No. 11, 1980, pp. 756–762.
- [4] Ward, I. M., *Mechanical Properties of Solid Polymers*, Wiley, 1979
- [5] Goel, A., Strabala, K., Negahban, M., and Turner, J. A., “Modeling the development of elastic anisotropy with plastic flow for glassy polycarbonate,” *Polymer Engineering and Science*, Vol. 49, No. 10, 2009, pp. 1951-1959.
- [6] Oh, H.-Y., Kim, B. H., “The effect of rolling orientation on the brittle-ductile transition in polycarbonate fracture,” *Polymer Engineering & Science*, Vol 26, No. 18, 1986, pp. 1290–1292.
- [7] Boyce, M. C., Arruda, E. M., and Jayachandran, R., “The large strain compression, tension, and simple shear of polycarbonate,” *Polymer Engineering and Science*, Vol. 34, No. 9, 1994, pp. 716–725.
- [8] Kolman, H. J., Ard, K., and Beatty, C. L., “Variation of dynamic mechanical properties of polycarbonate as a result of deformation,” *Polymer Engineering and Science*, Vol. 22, No. 15, 1982, pp. 950–954.
- [9] Liu, L. B., Yee, A. F., and Gidley, D. W., “Effect of cyclic stress on enthalpy relaxation in polycarbonate,” *Journal of Polymer Science Part B: Polymer Physics*, Vol. 30, No. 3, 1992, pp. 221–230.
- [10] Goel, A., Strabala, K., Negahban, M., and Feng, R., “Experimentally evaluating equilibrium stress in uniaxial tests,” *Experimental Mechanics*, Vol. 50, No. 6, 2009, pp. 709-716.
- [11] Bauwens-Crowet, C. and Bauwens, J.-C., “Rejuvenation and annealing effects on the loss curve of polycarbonate: 2. Cooling and ageing dependence,” *Polymer*, Vol. 31, No. 4, 1990, pp. 646–650.
- [12] Bauwens-Crowet, C. and Bauwens, J.-C., “Rejuvenation and annealing effects on the loss curve of polycarbonate: 1. Structural temperature dependence,” *Polymer*, Vol. 31, No. 2, 1990, pp. 248–252.

- [13] Othmezouri-Decerf, J., "Influence of mechanical deageing and subsequent physical ageing on the loss curve of polycarbonate," *Polymer*, Vol. 35, No. 22, 1994, pp. 4734–4742.
- [14] Thakkar, B. S. and Broutman, L. J., "Impact strength of polymers. 3: The effect of annealing on cold worked polycarbonates," *Polymer Engineering and Science*, Vol. 21, No. 3, 1981, pp. 155–162.
- [15] Broutman, L. J. and Krishnakumar, S. M., "Impact strength of polymers: 1. The effect of thermal treatment and residual stress," *Polymer Engineering and Science*, Vol. 16, No. 2, 1976, pp. 74–81.
- [16] Bubeck, R. A., Bales, S. E. and Lee, H.-D. (1984), "Changes in yield and deformation of polycarbonates caused by physical aging," *Polymer Engineering & Science*, Vol. 24, No. 14, 1984, pp. 1142–1148.
- [17] Ho, C. H. and Vu-Khanh, T., "Physical aging and time-temperature behavior concerning fracture performance of polycarbonate," *Theoretical and Applied Fracture Mechanics*, Vol. 41, No. 1-3, 2004, pp. 103–114.
- [18] Struik, L. C. E., *Physical Aging in Amorphous Polymers and Other Materials*, Elsevier, Amsterdam, 1978.
- [19] White, J. R., "Polymer ageing: physics, chemistry or engineering? Time to reflect," *Comptes Rendus Chimie*, Vol. 9, No. 11-12, 2006, pp. 1396–1408.
- [20] Grellmann, W. and Seidler, S., *Deformation and Fracture Behaviour of Polymers*, Springer, 2001.
- [21] Hodge, I. M., "Enthalpy relaxation and recovery in amorphous materials," *Journal of Non-Crystalline Solids*, Vol. 169, No. 3, 1994, pp. 211–266.
- [22] Rahouadj, R. and Cunat, C., *Physical Aging and Glass Transition of Polymers*, *Handbook of Materials Behavior Models*, Academic Press, Burlington, 2001, pp. 944–954.
- [23] Ho, C. H. and Vu-Khanh, T., "Effects of time and temperature on physical aging of polycarbonate," *Theoretical and Applied Fracture Mechanics*, Vol. 39, No. 2, 2003, pp. 107–116.
- [24] Delbreilh, L., Berns, A., and Lacabanne, C., "Secondary Retardation/Relaxation Processes in Bisphenol A Polycarbonate: Thermostimulated Creep and Dynamic Mechanical Analysis Combined Investigations," *International Journal of Polymer Analysis and Characterization*, Vol. 10, No. 1, 2005, pp. 41–56.

- [25] Ho, C. H. and Vu-Khanh, T., “Effects of physical aging on yielding kinetics of polycarbonate,” *Theoretical and Applied Fracture Mechanics*, Vol. 40, No. 1, 2003, pp. 75–83.
- [26] Heymans, N. and Rossum, S. V., “FTIR investigation of structural modifications during low-temperature ageing of polycarbonate,” *Journal of Materials Science*, Vol. 37, No. 20, 2002, pp. 4273–4277.
- [27] Hill, A. J., Katz, M., and Jones, P. L., “Isothermal volume relaxation in aged polycarbonate measured by positron annihilation lifetime spectroscopy,” *Polymer Engineering and Science*, Vol. 30, No. 13, 1990, pp. 762–768.
- [28] Hada, J., Slobodian, P., and Sha, P., “Volume and enthalpy relaxation response after combined temperature history in polycarbonate,” *Journal of Thermal Analysis and Calorimetry*, Vol. 80, No. 1, 2005, pp. 181–185.
- [29] Etienne, S., Hazeg, N., Duval, E., Mermet, A., Wypych, A., and David, L., “Physical aging and molecular mobility of amorphous polymers,” *Journal of Non-Crystalline Solids*, Vol. 353, No. 41-43, 2007, pp. 3871–3878.
- [30] ASTM E1820, Standard Test Method for Measurement of Fracture Toughness, 43. ASTM International.
- [31] ASTM D5045, Standard Test Methods for Plane-Strain Fracture Toughness and Strain Energy Release Rate of Plastic Materials, 51. ASTM International.